CHEMISTRY
A EUROPEAN JOURNAL

ChemPubSoc
Europe

DOI: 10.1002/chem.201203444

Molecular Spoked Wheels: Synthesis and Self-Assembly Studies on Rigid Nanoscale 2D Objects

A. Vikas Aggarwal,[a] Stefan-S. Jester,[a] Sara Mehdizadeh Taheri,[b] Stephan Förster,*[b] and Sigurd Höger*[a]

Abstract: We present the efficient synthesis of a new molecular spoked-wheel structure (**MSW-3**). Two derivatives with diameters of approximately 4 nm have been prepared. By highlighting the importance of pseudo-high-dilution conditions during cyclization, we were able to access the compounds on a several hundred milligram scale. In addition to the standard characterization (NMR spectroscopy, MS), we describe a detailed investigation of the optical properties of the fluorescent MSWs by comparison with appropriate model chromophores. Furthermore, a comprehensive study of the structure in solution by means of light- and X-ray scattering experiments has been conducted. Scanning tunneling microscopy (STM) revealed the two-dimensional organization of the molecules on highly oriented pyrolytic graphite and emphasized the spoked-wheel structure. The diameter of these molecules measured by small-angle X-ray scattering is in very good agreement with that obtained from STM and matches the results of molecular modeling. This confirms the rigidifying effect of the spokes, which results in highly shape-persistent nanometer-sized oblate organic compounds.

Keywords: aggregation · aromatic compounds · macrocycles · nanostructures · template synthesis

Introduction

Large oblate molecules that consist of arylene and alkynylene moieties have been in the focus of research since the 1960s and the 1970s, mainly with respect to the question about the aromaticity in cyclic conjugated π-systems (Figure 1).[1] After a period with only moderate scientific activity, the discovery of new carbon allotropes and the remarkable effort in the development of transition-metal-catalyzed C–C cross-coupling reactions reinitiated the interest in such carbon-rich compounds in the 1990s.[1a–d,h,2]

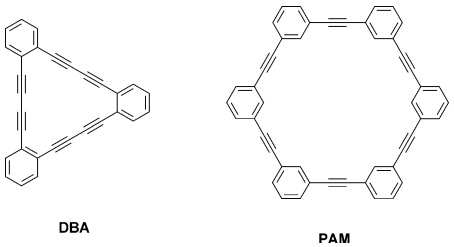

Figure 1. Chemical structures of dehydrobenzo[*n*]annulenes (DBAs) and phenylene–acetylene macrocycles (PAMs).

Although early publications on this topic focused on the basic concepts of macrocycle synthesis,[1a,d,e,2j,3] the attention soon shifted towards the investigation of the properties of the developed compounds.[2c,4] Nowadays, shape-persistent macrocycles (e.g., phenylene–acetylene macrocycles (PAMs) or dehydrobenzo[*n*]annulenes (DBAs)) are designed in advance to (ideally) possess desired and predictable molecular (microscopic), supramolecular (mesoscopic), and materials (macroscopic) properties and functionalities in light of their intended applications. In particular, the possibility to fine-tune the properties of the molecules by side-group modification has led to advanced systems. Recent efforts in the emerging field of molecular engineering have derived compounds that can act as optically active materials,[5] as molecular wires,[6] as containers for reactions in confined environments,[7] or as versatile tiles for surface patterning.[8] Nevertheless, although continuative fundamental research in the field of synthesis opens up new pathways to previously inaccessible compounds on larger scales, the investigations of inherent molecular and material properties still often lead to unexpected findings.[2a,5h,8i,9]

Recently, we reported about reinforced shape-persistent macrocycles, naming them molecular spoked wheels (MSWs), as their structures resemble a wheel-like motif (Figure 2).[10] We referred to their building blocks as hub, spokes, and rim, and this terminology shall be applied here as well. Apart from MSWs, only few macrocycles with rigid

[a] A. V. Aggarwal, Dr. S.-S. Jester, Prof. Dr. S. Höger
Kekulé-Institut für Organische Chemie und Biochemie
Rheinische Friedrich-Wilhelms-Universität Bonn
Gerhard-Domagk-Strasse 1, 53121 Bonn (Germany)
Fax: (+49) 228-73-5662
E-mail: Hoeger@uni-bonn.de

[b] S. M. Taheri, Prof. Dr. S. Förster
Physikalische Chemie I, Universität Bayreuth
Universitätsstrasse 30, 95440 Bayreuth (Germany)
E-mail: Stephan.Foerster@uni-bayreuth.de

Supporting information for this article is available on the WWW under http://dx.doi.org/10.1002/chem.201203444.

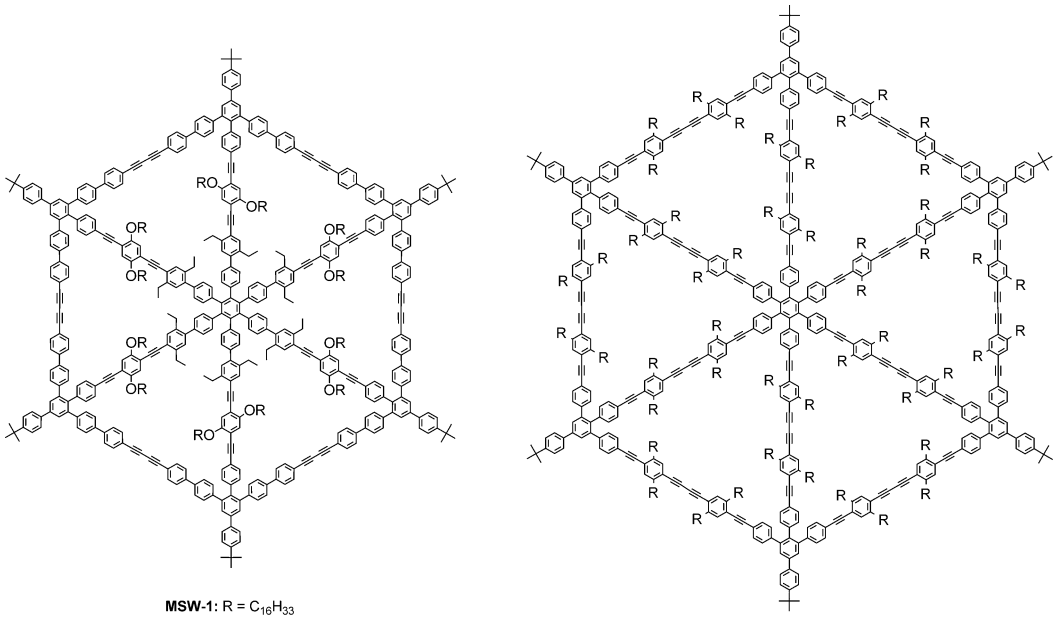

Figure 2. Previously synthesized **MSW-1** and **MSW-2a/b**.[10]

intraannular covalently attached moieties have been published to date.[11] The structure of the MSWs directly suggests that their synthesis can be performed by the covalent template approach.[2j,k,5b,12] Generally, covalent as well as noncovalent templates are often used in directed synthesis so as to favor the formation of a certain product or to increase yields.[2j,13] However, apart from solely acting as covalent connectors between the rim segments and the hub, thus facilitating a cyclization (instead of the otherwise expected formation of acyclic and cyclic oligomers of different oligomerization degrees), the spokes fulfill a second task: they also stiffen the final MSW structure by increasing the elastic modulus of the backbone. Although PAMs are often referred to as shape-persistent, molecular dynamics (MD) simulations indicate a high degree of flexibility of these structures in solution.[10b,12c] Even in crystal structures, distortions of the macrocyclic backbones are frequently observed[4,5i,14] and ascribed to the finite persistence length of poly(*p*-phenyleneacetylene)s (PPAs).[10b,15] This limited rigidity also becomes important when two-dimensional organization of the compounds is investigated.[8h] PAMs can be viewed as regular molecular polygons that consist of a tuple of corner units (i.e., implemented by *o*- or *m*-phenylene units or (hetero-) aromatic building blocks) that are linked by intermediate rigid rod units (i.e., realized by *p*-phenylene/acetylene units).[8h,16] When the polygons exceed a specific size or number of corner units (i.e., the circumference of the macrocycle exceeds a certain length), multiple conformations are possible, including collapsed ones. Consequently, such shape-persistent macrocycles can no longer be viewed as (truly) rigid. MSWs, on the other hand, can either be considered as, more descriptively, macrocycles that are reinforced by rigid spokes, or, probably more correctly, as six small fused triangular shape-persistent macrocycles. According to the first model, the spoke units of the MSWs restrict the conformational degrees of freedom of shape-persistent macrocycles, so that (apart from elasticity) their noncollapsed symmetrical shape is maintained even if the compounds are rather large. According to the second model, shape persistency is achieved by the fusion of (smaller) triangular macrocycles that reduce their degrees of freedom as distortions of any segment induce an additional strain on the other triangular parts of the MSW. For the first MSW (**MSW-1**), which had a diameter of 5–6 nm (depending on the atoms depicted for the distance measurement), extensive molecular dynamics (MD) and small-angle neutron scattering (SANS) experiments were conducted.[10b,12c] The MD trajectory, which shows the temporal evolution of the distance between two opposing atoms and their angle with the hub, revealed that the MSW is much more rigid than its uncyclized precursor or a corresponding PAM without rigidifying spokes.[10b]

Additional proof of the wheel-like structure of MSWs came from scanning tunneling microscopy (STM) investigations performed in situ at the liquid–solid interface. For both macrocycles **MSW-1** and **MSW-2**, submolecular features, the backbone, the hub, the six spokes, and the six rim segments were observable.[10a,b] Information on the self-assembly behavior of MSWs was obtained by atomic force microscopy (AFM), which revealed a strong dependency of the 3D packing of the MSWs on the length of their solubilizing side groups.[10a,b] In this context it is worth mentioning that **MSW-2a**, with 48 hexyl side chains, exhibits a strong tendency to form fiberlike structures when drop-casted from

toluene onto graphite. The resulting fibers extend over several hundred nanometers and consist of stacks of MSWs oriented perpendicularly to the surface.[10a] These results indicate that MSWs can aggregate even when they contain a rather large number of solubilizing side groups.

Herein, we present the synthesis of a new MSW (**MSW-3**) and highlight its molecular properties and its self-assembly in solution and on the surface. **MSW-3** is smaller, and therefore expected to be even more rigid than the previously reported **MSW**s (considering the molecular elasticity due to shorter rigid segments). Due to a straightforward synthetic protocol, **MSW-3a** was obtained on a scale of several hundreds of milligrams. This was a prerequisite for an investigation of further materials properties either in the pure state or as composite materials.[5k,17] **MSW-3b**, however, was constructed to allow subsequent functionalization after selective dealkylation of the *t*Bu periphery under mild acidic conditions.

Results and Discussion

Synthesis: Figure 3 shows the chemical structure of **MSW-3a** and **MSW-3b**. Both molecules are based on the same backbone but differ in their side-chain lengths. Their synthesis

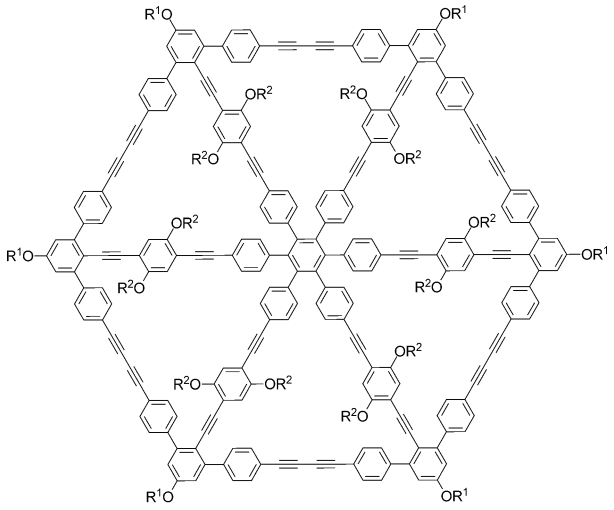

Figure 3. Chemical structure of the new MSWs.

relies on a convex modular approach:[10] the three distinct building blocks (the rim, spoke, and hub modules) are prepared independently from each other and are combined just prior to the cyclization (Figure 4). This minimizes the number of sixfold transformations during the synthesis.

Synthesis of the modules: The efficient preparation of the spoke/rim segment **10a/b** was a central task to the MSW synthesis (Scheme 1, top). Therefore two different routes to-

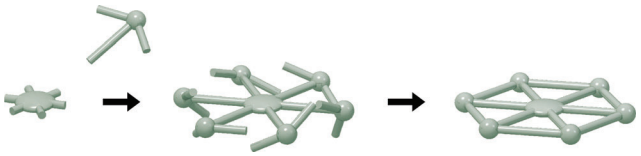

Figure 4. Schematic representation of the convex modular synthetic approach towards **MSW-3a/b**.

wards the rim module **7a** were studied. The first route began with the bromination of anisidine (**1**) followed by a twofold Suzuki coupling[18] of **2** with the boronic ester triisopropyl{[4-(4,4,5,5-tetramethyl-1,3,2-dioxaborolan-2-yl)phenyl]ethynyl}silane (see Figure S3 in the Supporting Information).[10b] Compound **3** was obtained after column chromatography and its amino group was converted to the iodide by the addition of iodine and *tert*-butyl nitrite to a solution of **3** in benzene at 0 °C.[19] However, yields over all three steps were low to moderate, and **7a** was obtained in an overall yield of 11 %. An alternative route to **7a** was based on Hart's terphenyl synthesis. In principle, this reaction allows the preparation of 2′-functionalized *m*-terphenyls in a single step from 1,3-dibromides or 1,3-dichlorides.[20] However, 1,3-dichloro-5-methoxybenzene (**5a**) required prefunctionalization to direct metalation to the 2-position. Otherwise a biphenyl was formed instead of the *m*-terphenyl **7a**.[21] Therefore, **5a** was iodinated with phenyliodine bis(trifluoroacetate) (PIFA). This yielded 3,5-dichloro-4-iodoanisole together with 3,5-dichloro-2-iodoanisole in a 3:1 ratio.[22] Despite the fact that both compounds were inseparable at the current stage, this product mixture was subjected to the Hart reaction. We found that slow, dropwise addition of a solution of **6a** in diethyl ether to a solution of 4-[2-(triisopropylsilyl)ethynyl]phenyllithium (prepared by the reaction of 1-bromo-4-(triisopropylsilylethynyl)benzene[23] with *t*BuLi) was crucial to obtain the coupled product in high yields after an iodine quench.[24,25] Both products, the terphenyl (**7a**) as well as the undesired biphenyl side product, were isolated in yields that corresponded to approximately 75 % conversion of the respective iodides. Thus, clearly, the initial lithium–iodine exchange proceeds very rapidly under these conditions[25,26] and overrides any *o*-directing tendencies of the methoxy group. Separation of both products was straightforward by column chromatography, and **7a** was isolated as a pure compound. In summary, the route towards **7a** based on the Suzuki coupling allows the purification of all intermediate compounds, however, the overall yield over three steps is low (Scheme 1a–c; 11 %). On the other hand, the route by means of the Hart reaction is considerably shorter than the first route[27] and allows the isolation of much larger quantities of **7a** (Scheme 1e,f; 48 %). Thus, **7b** was prepared only by the second route.

Compound **5b** was not commercially available but readily prepared by the reaction of 3,5-dichlorophenol (**4**) with isobutene.[28] Attempts to iodinate **5b** regioselectively with PIFA in the 2-position were still unsatisfactory, although a better regioisomer ratio of 6:1 was obtained as calculated

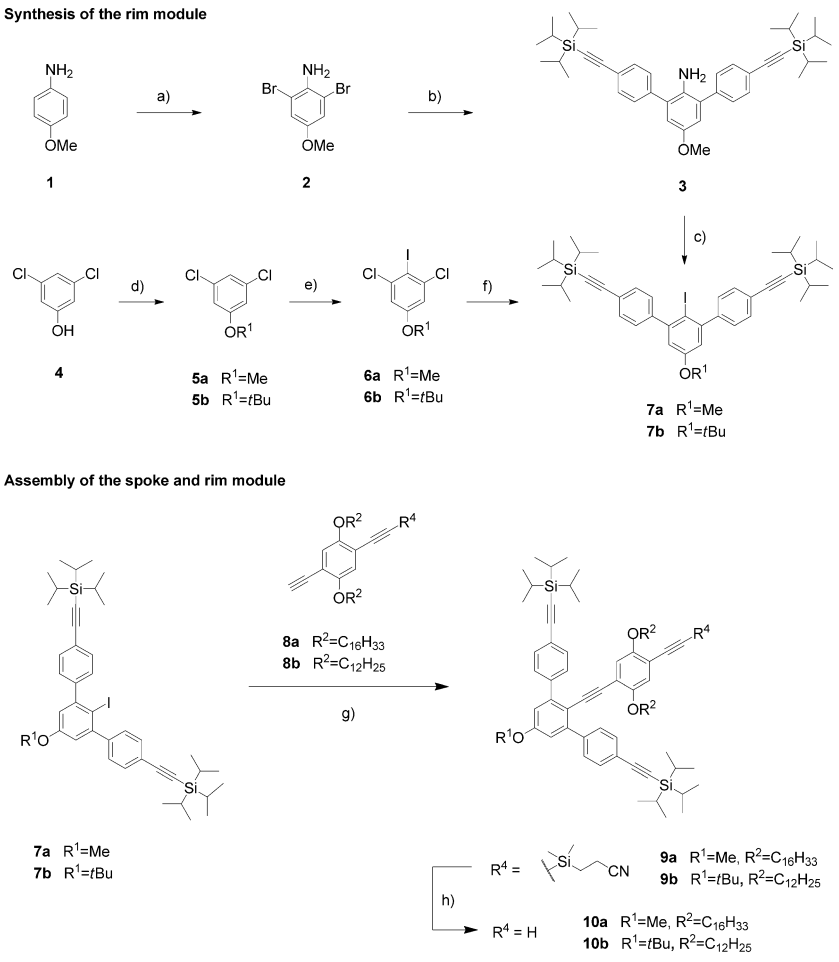

from the ^{1}H NMR spectrum of the crude reaction product. On the contrary, a clean synthesis of the desired 5-*tert*-butoxy-1,3-dichloro-2-iodobenzene (**6b**) was achieved by deprotonation of **5b** with *n*BuLi at −78 °C followed by the addition of iodine. In contrast to the methoxy group on **5a**, the *t*Bu group on **5b** is bulky enough to suppress any *o*-directing effects of the oxygen atom.[29] Hence, the most acidic hydrogen atom, located between both chlorine atoms, was substituted.[30] Compound **6b**, prepared by the latter route, was then converted to **7b** in a similar manner as described for the synthesis of **7a**. All in all, the yields of both **7a** and **7b** show that the Hart reaction opens up an efficient way towards functionalized *m*-terphenyls that can be incorporated into the spoked-wheel struc-

Scheme 1. Synthesis of **MSW-3a** and **MSW-3b**. a) Br_2, CH_2Cl_2, MeOH, 0 °C–RT, 4 h, 64 %; b) triisopropyl{[4-(4,4,5,5-tetramethyl-1,3,2-dioxaborolan-2-yl)phenyl]ethynyl}silane, pyridine-enhanced precatalyst preparation stabilization and initiation (PEPPSI), KOH, THF, 60 °C, 24 h, 47 %;[33] c) *t*BuONO, I_2, benzene, 0 °C–RT, 17 h, 36 %; d) R^1 = *t*Bu: 1) isobutene, F_3CSO_3H, CH_2Cl_2, −78 °C, 3 h; 2) NEt_3, −78 °C–RT, 17 h, 86 %; e) R^1 = Me: PIFA, I_2, CH_2Cl_2, RT, 2.5 h, 85 % (3:1 mixture); R^1 = *t*Bu: 1) *n*BuLi, THF, −78 °C, 90 min; 2) I_2, THF, −50–10 °C, 20 min, 90 %; f) 1) 1-bromo-4-(triisopropylsilylethynyl)benzene, *t*BuLi, Et_2O, −78–10 °C, 1 h; 2) **10**, 10 °C–RT, 17 h; 3) I_2, Et_2O, 0 °C, 60 min; **7a**: 73 %/48 % (over two steps: e + f); **7b**: 66 %; g) [$PdCl_2(PPh_3)_2$], CuI, PPh_3, THF, piperidine; **9a**: 90 °C, 3.5 h, 75 %; **9b**: μw (microwave irradiation), 120 °C, 12 min, 81 %; h) K_2CO_3, THF, methanol, RT, 2 h; **10a**: 91 %; **10b**: 94 %; i) [$PdCl_2(PPh_3)_2$], CuI, PPh_3, THF, piperidine, 80 °C, 17 h; **11a**: 76 %; **11b**: 77 %; j) TBAF, THF, 0 °C–RT, 3 h; **12a**: 98 %; **12b**: 74 %; k) addition of **12a/b** to a stirred solution of [$PdCl_2(PPh_3)_2$], CuI, I_2, $NHiPr_2$, THF, 50 °C; **MSW-3a**: 90 h, 79 %; **MSW-3b**: O_2, 48 h, 68 %. HIPB = hexa(4-iodophenyl)benzene.

tures as shown below. The spoke (**8a/b**) and hub (hexa(4-iodophenyl)benzene (HIPB)) modules were readily obtained by adopting procedures known from the literature (details are reported in the Supporting Information).[31]

Assembly of the modules: The spoke module **8a** and the corner piece **7a** were linked by a Sonogashira–Hagihara reaction (Scheme 1, middle). With $[Pd(PPh_3)_2Cl_2]$, copper iodide, and triphenylphosphane as catalyst system,[32] it was essential to conduct this reaction at an elevated temperature of at least 80 °C although the coupling of the acetylene was performed with an aryl iodide. Lower reaction temperatures only led to the formation of the diacetylene coupling product, most probably owing to the steric hindrance at the iodo position of **7**. Nevertheless, **9a** could be obtained in 80% yield. In contrast, the yields of **9b** were considerably lower when using the same reaction conditions (Table 1).

Table 1. Variations of the conditions of the Sonogashira–Hagihara reaction towards **9b**.

Entry	Catalyst system	Solvent	Base	Heat[a]	*t*	Yield [%]
1	$[Pd(PPh_3)_2Cl_2]$ PPh_3, CuI	THF	piperidine	conv 90 °C	17 h	31
2	$[Pd(PPh_3)_2Cl_2]$ PPh_3, CuI	THF	piperidine	μw 120 °C	12 min	77
3	$[PdCl_2(dppe)]$ CuI[d]	–	piperidine	μw 120 °C	10 min	–
4	$[Pd(MeCN)_2Cl_2]$ $PtBu_3$, CuI[34]	THF	piperidine DBU[b]	μw 120 °C	12 min	30[35]
5	$[(AllylPdCl_2)_2]$ $PtBu_3$[36]	MeCN	piperidine DABCO[c]	μw 120 °C	12 min	12

[a] μw = Microwave irradiation, conv = conventional heating. [b] DBU = 1,8-diazabicycloundec-7-ene. [c] DABCO = 1,4-diazabicyclo[2.2.2]octane. [d] dppe = 1,2-bis(diphenylphosphino)ethane.

However, microwave (μw) heating of a sealed system resulted in a dramatic increase of the product yield, and the reaction time was reduced to a few minutes. By using the standard catalyst system and heating to 120 °C in a sealed vessel, **9b** was obtained in yields comparable to those of **9a** (Table 1, entry 2). At present, we ascribe this observation to the much higher reaction temperature (120 °C) that is obtainable in the sealed microwave flask.[37] A further variation of the reaction conditions (ligand, base) only gave inferior product yields (Table 1).

The 3-(cyanopropyl)dimethylsilyl (CPDMS) protecting groups on **9a** and **9b** were removed selectively.[38] Similarly to the trimethylsilyl (TMS) group, CPDMS is readily cleaved by potassium carbonate in THF/MeOH, thus leaving the more stable triisopropylsilyl groups (TIPS) unaffected (**10a/b**). Subsequently, **10a** and **10b** were coupled to the hub module (HIPB) in a sixfold Sonogashira–Hagihara reaction.[10a] By employing $[Pd(PPh_3)_2Cl_2]$, copper iodide, and triphenylphosphane at 80 °C, excellent yields of 76 and 77% were obtained, which corresponded to 96% conversion per reactive site. Then all twelve TIPS groups of **11a/b** were removed in good to excellent yields with tetrabutylammonium fluoride (TBAF) in THF within 3 h at RT (**12a/b**; Scheme 1, middle).[39]

Cyclization reaction: Cyclization reactions (Scheme 1, bottom) of **12a** and **12b** to **MSW-3a** and **MSW-3b**, respectively, were performed by very slow addition of diluted solutions of **12a/b** in THF to vigorously stirred solutions of the catalyst systems ($[Pd(PPh_3)_2Cl_2]$, CuI, co-oxidizing agent)[9a] in THF and di(isopropyl)amine at 50 °C. For the cyclization of **12a**, I_2 was employed as the co-oxidizing agent, and the dependency of the product yield on the time of addition and concentration was investigated. In a second optimization step, alternative (co-)oxidizing agents were tested on the cyclization of **12b**.

The template effect of the hub/spoke system on **12a/b** strongly favors intramolecular cyclization. Nevertheless, the molecular-weight distribution of the crude product of **MSW-3a** heavily depends on the addition time and on the concentration, as determined by gel permeation chromatography (GPC) analysis (Figure 5a). If **12a** (0.83 μmol, 5 mg, 2 mL solution) is added instantly to a concentrated solution of the catalyst (1.4 equiv $[PdCl_2(PPh_3)_2]$, 2.0 equiv CuI, 7.8 equiv I_2, 2.5 mL solution; thus resulting in a concentration of **12a** of 184 μmol L^{-1}), a large amount of dimer and even higher oligomers are produced. Increasing the time of addition to 117 h and reducing the concentration of **12a** in the receiver to 0.2 μmol L^{-1}[40] gives the desired molecular spoked wheel almost exclusively. These findings underline the importance of (pseudo) high-dilution conditions[3] for the success of multiple intramolecular coupling reactions, even for templated PAMs.

To enable the preparation of large quantities of **MSW-3a/b**, the reduction of the amount of side products and of the reaction time were desired. As the copper-catalyzed protocol that had been optimized for the MSWs published earlier[10a] gave no conversion of the starting material (Figure 5b, light blue trace), modifications were made to the palladium-based catalyst system. Since a rate increase of the coupling reaction would have the same effect as a slower reactant addition, alternative co-oxidizing agents were considered for the cyclization reaction of **12b** (Figure 5b). In fact, bubbling air through the solution prior to the reaction or employing benzoquinone or 2,3-dichloro-5,6-dicyano-1,4-benzoquinone (DDQ) instead of iodine under an inert atmosphere proved beneficial for the intramolecular reaction. The amount of dimer formed was reduced to a third.[41]

The total yield over the final five steps in which the modules **7a**, **8a**, and HIPB were assembled reached up to 40% for this macrocycle. Thus, on account of the efficient synthetic route, we were able to obtain nearly 400 mg of **MSW-3a**.

Proof of cyclization: The successful sixfold ring closure was proven by a variety of analytical methods. GPC shows an in-

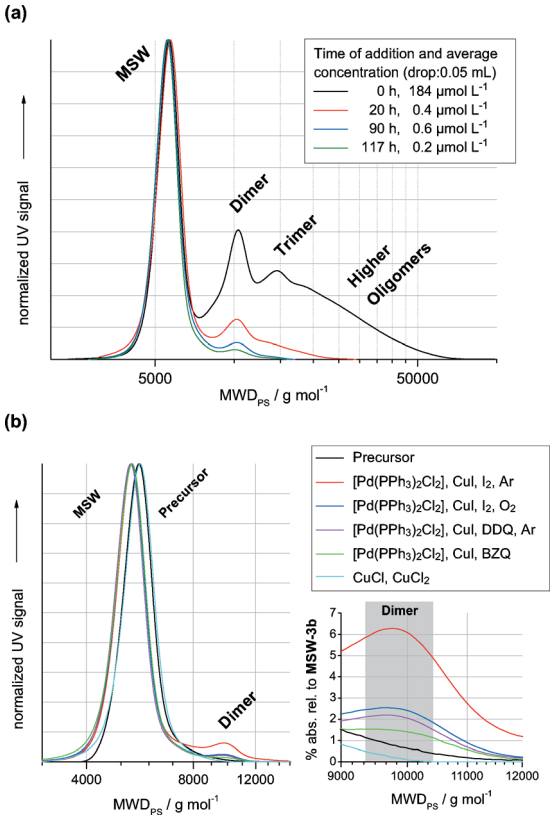

Figure 5. a) Dependency of the relative amounts of **MSW-3a**, related dimer, and higher oligomers on the concentration of **12a** in the reaction flask and the time of addition (catalyst: $[PdCl_2(PPh_3)_2]$, CuI, I_2, diisopropylamine, THF). Apart from the instant addition, the concentrations were calculated for an assumed drop size of 0.05 mL.[40] b) Left: Amounts of **MSW-3b** and the corresponding dimer relative to the type of oxidizing agent used. These reactions were performed by instant addition of a solution of **12b** to the heated catalyst solution, thereby resulting in an initial concentration of 28 μmol L^{-1}. Right: Magnification of the dimeric by-product peak (UV absorption at 254 nm) in relation to the peak of **MSW-3b**. DDQ = 2,3-dichloro-5,6-dicyano-1,4-benzoquinone; BZQ = benzoquinone; DBU = 1,8-diazabicycloundec-7-ene.

crease in retention time upon cyclization of **12a/b** to **MSW-3a/b** that corresponds to a reduction of the estimated molecular mass of approximately 325 Da instead of 12 Da expected for the loss of twelve hydrogen atoms. However, GPC is a relative method for the detection of molecular weights with a calibration based on the assignment of a measured retention time to a specific molecular weight, in our case a narrow dispersed polystyrene (PS) standard. The overestimated molar mass difference between **12a/b** and **MSW-3a/b** is ascribed to the reduced hydrodynamic radius of the MSW relative to the open precursor. In **MSW-3a/b** the rim–spoke–"arms" are fixed in a plane and are therefore not nearly as space filling as in **12a/b** in which they can rotate around the spoke axis and also bend out of the plane. In addition, the underestimation of the molecular weight by GPC increases with the length of the alkyl chains. This is consistent with expectations for branched molecular objects with a high graft density. Conversely, the spoked-wheel backbone is more rigid than polystyrene, and its hydrodynamic radius expands faster than that of a coiled polymer (such as PS) but not nearly as fast as for linear rigid rod molecules.[42] The combination of both effects leads to a rather good agreement between GPC-measured (PS calibration) and exact molecular weight (Table 2).

Table 2. Comparison of GPC-determined (PS calibration; peak molecular weight) and exact molecular weights.

Compound	M_{abs} [g mol^{-1}]	M_{GPC} [g mol^{-1}]	M_{GPC}/M_{abs}
12a	6002.76	5830	0.97
MSW-3a	5990.66	5510	0.92
12b	5581.96	5620	1.01
MSW-3b	5569.86	5290	0.95

Matrix-assisted laser desorption/ionization mass spectrometry (MALDI-MS) clearly shows a difference of 12 Da that corresponds to the twelve terminal acetylene hydrogen atoms (Table 2). Furthermore, their absence at $\delta = 3.1$ ppm is observed by ^{1}H NMR spectroscopy. Even the signals in the aromatic region are well resolved and can be assigned unambiguously (Figure 6).

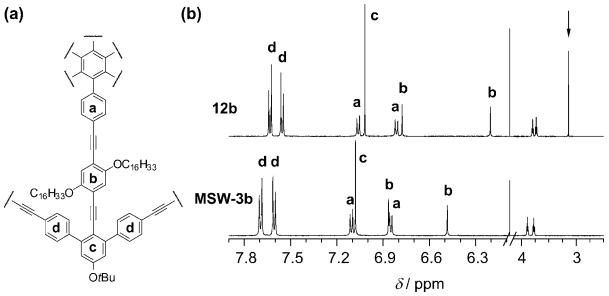

Figure 6. a) Partial molecular structure of **12b** and **MSW-3b**, including an assignment of the ^{1}H NMR spectroscopic signals to hydrogen atoms of the aromatic building blocks. b) ^{1}H NMR spectra of **12b** and **MSW-3b**. The absence of the acetylene signal at $\delta = 3.1$ ppm (see arrow) in **MSW-3b** is a clear indicator of an effective cyclization.

Optical properties: The UV/Vis absorption and emission spectra of corresponding compounds (**MSW-3a/b** and **12a/b**) are very similar, although the absorption spectrum of **12b** shows a better resolved fine structure than the spectrum of **12a** (see the Supporting Information for the spectra of **12a**, **MSW-3a**, **12b**, and **MSW-3b**; the former are also included in Figure 8 below).

To model the UV/Vis absorption spectrum of **12a**, different chromophores were combined to model sets. Scheme 2 outlines the synthesis of the chromophores that is based on repetitive Sonogashira–Hagihara coupling and acetylene deprotecting reactions. Compound **15** resembles the rim chromophore of **12a** omitting the methoxy and phenyl groups in *m* positions, as π-conjugation is expected to be hindered.[10a,43] Compounds **20** and **22** represent the spoke chromophore. Whereas **20** considers the expected interruption of

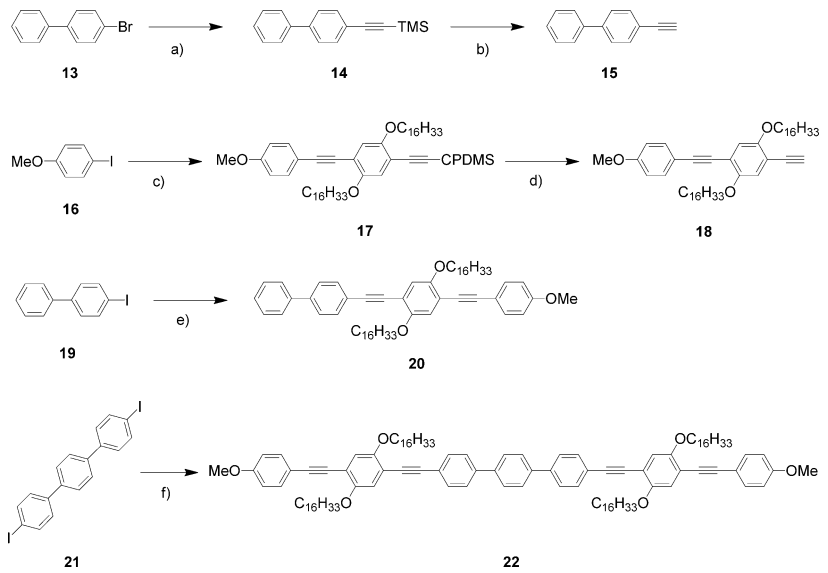

Scheme 2. Synthesis of the model chromophores. a) TMSA, $[PdCl_2(PPh_3)_2]$, CuI, PPh_3, THF, piperidine, 120 °C, 12 min (μw), 85 %; b) K_2CO_3, THF, methanol, RT, 2 h, 92 %; c) **8a**, $[Pd_2(dba)_3]$, CuI, dppf, THF, piperidine, 40 °C, 17 h, 82 %; d) K_2CO_3, THF, methanol, RT, 2 h, 71 %; e) **18**, $[Pd_2(dba)_3]$, CuI, dppf, THF, piperidine, 120 °C, 12 min (μw), 77 %; f) $[PdCl_2(PPh_3)_2]$, CuI, PPh_3, THF, piperidine, 120 °C, 12 min (μw), 72 %. CPDMS = (3-cyanopropyl)dimethylsilyl.

conjugation along the spoke by a turbine-like arrangement around the central hub, compound **22** spans the whole width of the macrocycle. By an appropriate combination of these chromophores, various model sets were prepared for **12a**. Two of them will be discussed here. In agreement with the model for **MSW-2**, model system 1 contains six of the short chromophores (**20**). Instead, model system 2 includes three spoke chromophores (**22**). To model the rim units, both contain twelve 4-ethynyl-1,1′-biphenyl (**15**) units. Figure 7 shows comparisons between the absorption spectra of precursor **12a** and both model systems.

Clearly, the absorption cannot be explained by purely adding up the extinction coefficients of the chromophores. The absorption of precursor **12a** at 384 nm is only about 60 % of that of the model systems. To simplify the comparison of the relative shifts, Figure 7b shows the precursor as well as the model systems normalized to the second absorption maximum ($\lambda = 384$ nm for **12a** and model 2, and $\lambda = 374$ nm for model 1). The left-hand side of the absorption spectrum is determined by the absorption of the rim module, though the use of only one chromophore type is not sufficient. The right-hand side of the spectrum is defined by the absorption of the spoke chromophore. Clearly—and contrary to earlier results[10a]—the spoke chromophore is not divided in two halves by the hexaphenylbenzene hub. Here, a coupling of the π-conjugation of the chromophores across the hub is necessary to explain the absorption spectrum of **12a**.

Upon cyclization, distinctive changes in the UV/Vis absorption spectra can be observed (Figure 8). The intensity of the previously most prominent absorption features, namely, the absorption in the region of 250 nm $< \lambda <$ 300 nm as well as the absorption derived from the extended spoke chromophore ($\lambda_{max} = 384$ nm) decrease. Instead, two new absorption maxima are observed at $\lambda = 323$ and 345 nm.

These changes are attributed to two processes. Firstly, the length doubling of the rim chromophore after the acetylene homocoupling leads to a strong redshift of the previously unresolved features with $\lambda < 300$ nm (the absorption spectrum of 1,4-bis[4-(1,1′-biphenyl)]butadiyne ($\lambda_{max} = 332$ nm) can be found in the Supporting Information). Secondly, the cyclization constrains the rotational degrees of freedom of the phenyl units on the spoke and hub modules. As a result, the intensity of the band at $\lambda = 384$ nm is reduced, and a hypsochromic shift of the spoke chromophore is observed.[44] Nevertheless, the long chromophore can still be observed as a shoulder in the absorption spec-

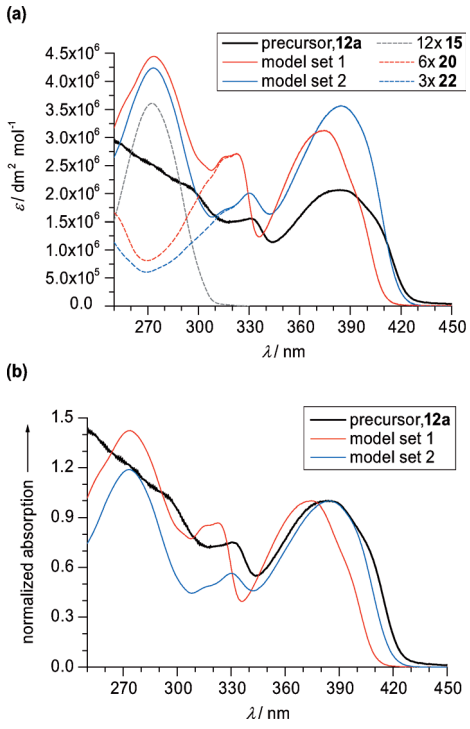

Figure 7. a) Comparison of the UV/Vis absorption spectra of **12a** (CH_2Cl_2, 6.7×10^{-6} mol L^{-1}) with its two model systems composed of 12 × **15** (CH_2Cl_2, 1.0×10^{-5} mol L^{-1}) and either 6 × **20** (CH_2Cl_2, 5.0×10^{-6} mol L^{-1}) (model system 1) or 3 × **22** (CH_2Cl_2, 5.0×10^{-6} mol L^{-1}) (model system 2). b) Comparison of the normalized UV/Vis absorption spectra of **12a** and both model systems.

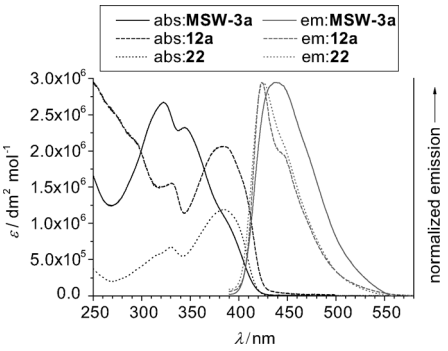

Figure 8. Comparison of the absorption (black) and emission (gray) spectra of **12a** (dashed; for abs: CH_2Cl_2, 6.7×10^{-7} mol L^{-1}; for em: CH_2Cl_2, 3.4×10^{-8} mol L^{-1}), **MSW-3a** (solid; for abs: CH_2Cl_2, 1.8×10^{-6} mol L^{-1}; for em: CH_2Cl_2, 9.0×10^{-8} mol L^{-1}) and **22** (dotted; for abs: CH_2Cl_2, 5.0×10^{-6} mol L^{-1}; for em: CH_2Cl_2, 2.5×10^{-7} mol L^{-1}). A color version of this plot containing the spectra of **20** is included in the Supporting Information.

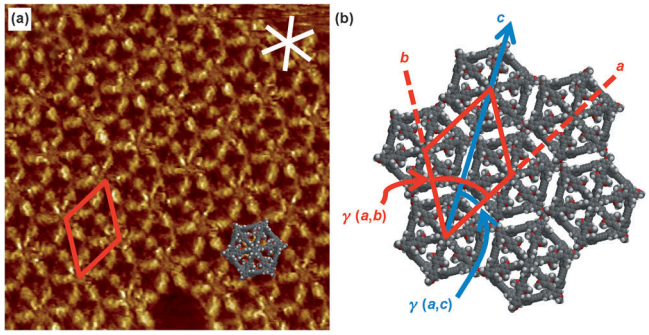

Figure 9. a) STM image of a self-assembled monolayer of **MSW-3a** at the 1-octanoic acid/HOPG interface (25.0×25.0 nm^2; $V_S=-1.5$ V; $I_t=5$ pA); b) supramolecular monolayer model. A unit cell of $a=(4.1\pm0.1)$ nm, $b=(4.1\pm0.1)$ nm, and $\gamma(a,b)=(60\pm1)°$ is indexed. The spoke units are aligned along c_n with $\gamma(a,c_n)=30°+n\times60°$; $n=$integer. The red, white, and blue lines indicate the unit cell, HOPG main axis directions, and the spoke directions, respectively. Note: The hexadecyloxy side chains are not adsorbed onto the substrate and are thus neglected in the molecular model in (b).

trum of **MSW-3a**. In fact, the maximum of the emission spectrum (Figure 8) is redshifted by 12 nm in the MSW with respect to the open precursor **12a**. At the same time, the emission spectrum of the MSW is very broad and shows no distinct features. Considering almost identical emission spectra of **12a** and **22**, we conclude that in both cases **22** is likely to be the longest chromophore present.

Self-assembly studies at the solid/liquid interface: To optimize the MSWs for applications in material science it is important to analyze their structures in solution as well as on surfaces and at interfaces. The long hexadecyloxy chains were introduced to shield the unsaturated moieties, hence, to reduce π-stacking and to guarantee a high solubility.[45] As a result, **MSW-3a** and **MSW-3b** are highly soluble in CH_2Cl_2, THF, and toluene (even more than 10 wt%), whereas the solubility in pure hexane or methanol remains low. Owing to steric reasons, **MSW-3a** and **MSW-3b** force the largest parts of the alkoxy chains to be oriented orthogonal to the ring plane into the solvent phase. Therefore, both compounds were barely expected to form monolayers on highly oriented pyrolytic graphite (HOPG).[46] However, for **MSW-3a** we could observe two-dimensional self-assembly at the interface of 1-octanoic acid and HOPG by STM (see Figure 9a). The molecules form a highly ordered pattern, and a hexagonal unit cell of $a=(4.1\pm0.1)$ nm, $b=(4.1\pm0.1)$ nm, and $\gamma(a,b)=(60\pm1)°$ was indexed. The sixfold symmetry of the brightly appearing rigid-rod units ("spokes") can be clearly observed. The lattice parameters of the hexagonal pattern are consistent with the shape and size of the molecular backbone (see Figure 9b), whereas the methoxy substituents at the outer corners define the intermolecular distances of the rim rod units. The hexadecyloxy side chains are not observable and are most probably not adsorbed to the substrate, but rather point to the solution phase.

Self-assembly studies in solution: Neither the UV/Vis absorption spectrum (in CH_2Cl_2 over a concentration range from 1×10^{-7} to 1×10^{-4} mol L^{-1}) nor the ^{1}H NMR spectrum (in [D$_3$]chloroform over a concentration range from 0.5 mg mL^{-1} (8.3×10^{-5} mol L^{-1}) to 27 mg mL^{-1} (4.4×10^{-3} mol L^{-1})) of **MSW-3a** were concentration-dependent (the spectra are included in the Supporting Information). However, these studies are not sufficient to gain insight into the solution on a molecular level.

Dynamic light scattering (DLS) is especially sensitive to large particles (scattering intensity scales with approximately R_h^6, in which $R_h=$hydrodynamic radius),[47] thus allowing the determination of very low concentrations of aggregates. Therefore, chloroform and toluene, which form clear solutions even at weight contents of 10 wt% of **MSW-3a**, were chosen for the evaluation of its solubility. The measurements were conducted at concentrations of 1 mg mL^{-1} (which corresponds to 0.1 wt% in toluene and 0.07 wt% in chloroform) and 6 mg mL^{-1} (which corresponds to 0.7 wt% in toluene and 0.4 wt% in chloroform). CONTIN[48] (Figure 10a) as well as cumulant (Figure 10c) analysis reveal almost exclusively the monomer in the solutions in toluene (magenta and cyan curves), whereas the aggregate accounts for 45% of the scattered light intensity in the dilute chloroform solution (Figure 10a, green curve). Although this distribution is stable over time (Figure 10c), the aggregation process can be monitored at higher concentrations (Figure 10b). For this solution (6 mg mL^{-1} in $CHCl_3$) the semilogarithmic plot of the first cumulant reveals the presence of two regions with very different behavior (Figure 10c). For $t<100$ min, aggregation to large particles is very fast but slows down considerably afterwards. By stretching the timescale by logarithmic plotting (Figure 10d), a linear behavior for $t<80$ min and a crossover region until about 300 min is observed, followed by a linear behavior, now at a reduced rate of aggregation.

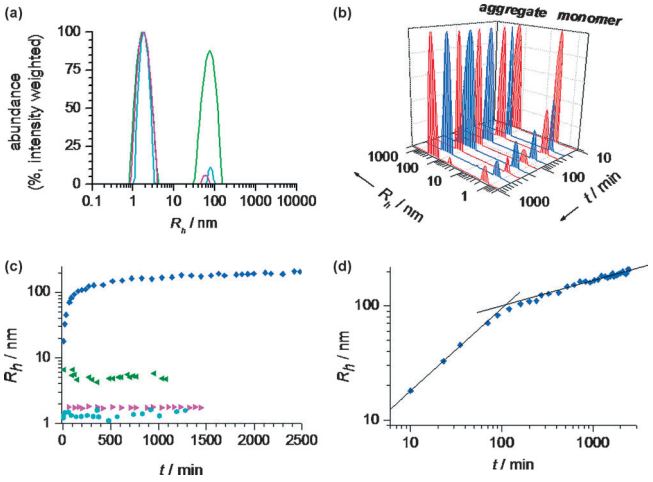

Figure 10. a) CONTIN analysis of solutions of **MSW-3a** in chloroform (1 mg mL^{-1} (green), after 21 h) and in toluene (1 (turquoise) and 6 mg mL^{-1} (magenta) after 28 and 25 h, respectively). b) CONTIN analysis of a solution of **MSW-3a** in chloroform (6 mg mL^{-1}) at different times (succeeding curves have been colored in blue and red for clarity). c) Cumulant analysis: semilogarithmic plot with linear time axis (chloroform: 1 (green) and 6 mg mL^{-1} (blue); toluene: 1 (turquoise) and 6 mg mL^{-1} (magenta)) and d) logarithmic plot of the concentrated sample in chloroform (blue, 6 mg mL^{-1}) with lines (black, not fitted) emphasizing the linear behavior for $t<80$ min and $t>300$ min obtained from a cumulant analysis. All values were calculated from autocorrelation curves recorded at an angle of 30° at 25 °C.

The change in kinetics can also be observed directly by comparison of the normalized autocorrelation curves (Figure 11a,b). Over the whole time span, bimodal relaxation curves are recorded; these correspond to one fast (small particle, monomer) and one slow (large particle, aggregate) relaxation process. Whereas the first 120 min are characterized by the fast rise of the exponential that corresponds to the slow process, it stagnates until about 270 min have passed (Figure 11a), before it begins to decrease slightly, whereas the autocorrelation curve shifts towards larger relaxation times (Figure 11b). The integration of the CONTIN distribution, as well as double-exponential fitting to the autocorrelation curves (details are shown in the Supporting Information), give a more differentiated view. After the fast initial aggregation phase, the ratio of aggregate to monomer begins to decrease slightly, whereas the aggregate size continuously grows. Figures 11c,d show the corresponding plots versus time. The observed behavior is probably the result of the reorganization of initially formed thermodynamically unstable aggregates to more regular self-assembled structures.[49] Considering the abundance of monomers and rather large aggregates at all times, it can be concluded that self-assembly follows a cooperative aggregation mechanism that involves an energy barrier for dimerization.[50] In terms of solvent quality, chloroform and toluene can be distinguished clearly. Whereas chloroform leads to association even at a concentration of 1 mg mL^{-1} (though never visible by the bare eye), toluene is a much better solvent for these systems.

Small-angle X-ray scattering (SAXS): As mentioned above, the DLS experiments of solutions in chloroform indicated the formation of aggregates. To gain a deeper insight into their structure, SAXS measurements were performed. Owing to the strong X-ray absorption of chloroform, SAXS studies in respective solutions were not possible. However, measurements in toluene could be performed over a range of concentrations (2.5, 5, and 10%) in the dilute regime. Figure 12 shows the measured SAXS curves for the three solutions.

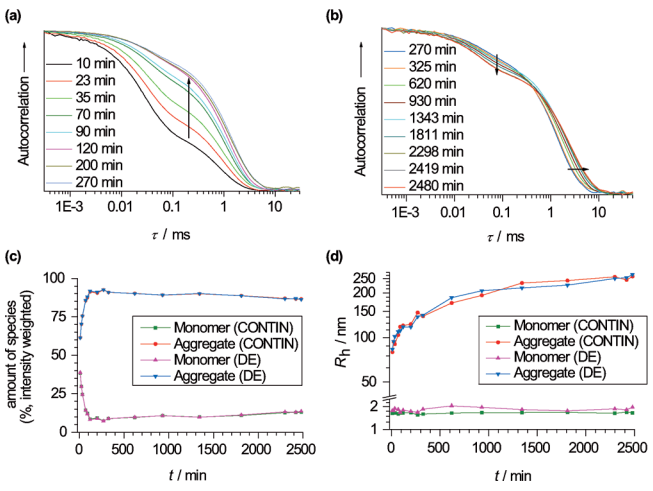

Figure 11. Detailed analysis of the aggregation of the **MSW-3a** sample in chloroform (6 mg mL^{-1}, angle: 30°, $T=25$ °C). a,b) Autocorrelation curves (scattering angle: 45°) after a) 10–270 min and b) 270–2480 min. c,d) Results from CONTIN analysis and double-exponential (DE) fitting to the autocorrelation curves: c) Ratio of monomer to aggregate versus time; d) sizes of aggregate and monomer versus time.

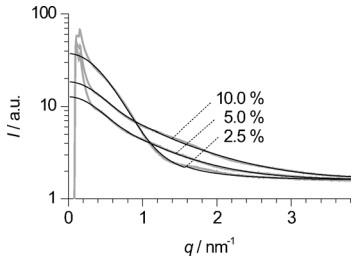

Figure 12. SAXS curves measured (gray) for **MSW-3a** at concentrations of 2.5, 5, and 10% in toluene with appropriate model curves (black). The SAXS curve at 2.5% can be described by short disk stacks, whereas at concentrations of 5 and 10% the scattering curves can be thoroughly described by core–shell cylinders.

The black lines are fits to simple geometrical structures. At a concentration of 2.5% the scattering curve can be quantitatively described by a disk with a radius of 3.2 nm and a thickness of 0.6 nm. The measured radius is somewhat larger than the geometrical radius estimated from Figure 9. This indicates some aggregate formation, although not yet

with a well-defined cylindrical structure. At the two higher concentrations (5 and 10%), the scattering vector (q) dependence of the measured scattering curves differ considerably from the q dependence of the scattering curve measured at lower concentration. Both scattering curves can be described by a core–shell cylinder with a core radius of 0.9 nm, an overall radius of 1.7 nm, and a length of 25 nm. As the spatial resolution of the experiment is limited by the minimum q value, this length represents a lower limit. The fit to the scattering curve is not very sensitive to the core radius, but in reasonable agreement with aromatic core region of the molecules. The outer radius is in good agreement with geometrical radius of a cylindrical stacking of the molecules estimated from Figure 9 and confirms the preservation of the noncollapsed planar structure of the MSW in solution.

A sample in the dry state was also investigated by small-angle X-ray scattering to characterize the self-assembly behavior in the bulk. The SAXS curve shows several reflections, in which the first-order peak (10) is part of a set of peaks (11, 20) that are consistent with a hexagonal packing of cylinders (Figure 13). The corresponding cylinder–cylinder distance of 4.1 nm is in very good agreement with Figure 9. The two additional reflections at $q=2.45$ and 2.85 nm^{-1} (2.6 and 2.2 nm, respectively) are due to additional positional correlations of molecules within the cylinders or correlations of molecules in different (adjacent) cylinders, but cannot be indexed on any of the two-dimensional space groups.

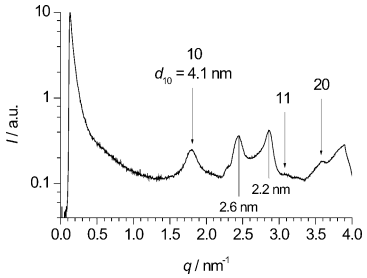

Figure 13. SAXS curve of **MSW-3a** in the dry state. The first-order peak (10) is part of a set of peaks that are consistent with a hexagonal packing of cylinders. The corresponding cylinder–cylinder distance of 4.1 nm is in very good agreement with Figure 9.

Thus the SAXS experiments confirm that rigid molecular spoked wheels self-assemble into well-defined rigid cylindrical structures, in solution as well as in the bulk, whereby the cylinders assemble into a hexagonal lattice.

Conclusion

In conclusion, we have developed and optimized a highly efficient synthetic route to molecular spoked wheels. The shape-persistent backbones resemble disklike platelets with diameters of approximately 4 nm substituted with twelve alkoxy side chains that point away from the latter. The synthesis is based on a modular convex template approach. The rim module has been prepared by a Hart reaction that has been optimized for the synthesis of functionalized alkoxy-containing terphenyls.[51] Furthermore, the cyclization step has been investigated in detail. To optimize MSWs for future applications in materials science, we closely looked into the structure of **MSW-3a** in solution and on surfaces. **MSW-3a** forms a close-packed 2D hexagonal lattice on HOPG as observed by STM. The self-assembly process in solution was investigated by DLS and SAXS. We concluded a cooperative mechanism with a fast initial self-assembly process followed by a slower reorganization of the aggregates. Furthermore, the shape and dimensions of the self-assembled structures were derived from SAXS measurements and are in good agreement with the findings from STM. Moreover, we were able to obtain MSWs in quantities that were sufficient to initiate investigations on advanced materials. Currently, the applicability of **MSW-3a** and derivatives thereof in high-performance nanocomposites are under investigation.

Experimental Section

STM: The experimental setup consisted of an Agilent 5500 SPM system placed on a Halcyonics active vibration damping platform and was surrounded by a home-built acoustic damping box. Mechanically cut Pt/Ir (80:20) tips were used and further modified in situ by applying short voltage pulses. Highly oriented pyrolytic graphite (HOPG) substrates were obtained from MikroMasch in ZYB quality and freshly cleaved prior to each experiment. All STM measurements were performed in situ (with the tip immersed into the liquid) and typically completed within 30 min after the sample preparation. As a representative experiment, 1 μL of a 10^{-5}–10^{-6} M solution of the respective substance in 1-octanoic acid was dropped onto freshly cleaved HOPG at an elevated temperature (80 °C), the temperature was retained for 30 s, and the sample was subsequently allowed to cool to RT prior to STM imaging. Bias voltages between −0.8 and −1.8 V and current set points between 2 and 30 pA were applied to image the molecular adlayers. All images were calibrated by subsequent immediate acquisition of an additional image at reduced bias voltage, therefore the atomic lattice of the HOPG surface is visible and can be used as a calibration grid. Data processing, also for image calibration, was performed using the SPIP 5 (Image Metrology) software package.

SAXS: SAXS was performed using a rotating anode setup (Seifert) that consisted of a rotating Cu anode (Rigaku), a Göbel mirror, and image plate detectors (Fuji) with a sample detector distance of 1.00 m. The experimental data were reduced and analyzed using the Scatter software.[52] Details of the structure and form factors and fitting procedures can be found in the literature.[53]

DLS: The measurements were conducted using an ALV-CGS-3 system with a He:Ne laser (632.8 nm) and an ALV/LSE-5004 autocorrelator. The temperature was regulated using a Thermo Haake Phoenix II theromostat and set to 25 °C for all measurements. All samples were prepared in a flow box to ensure a dust-free working environment. Hellma Analytics 540.110-QS cuvettes (inner diameter 8 mm, $V=2.8$ mL) were flushed with distilled acetone and allowed to dry overnight at RT. The samples were then dissolved in freshly distilled solvents and filtered through hydrophobic Rotilabo syringe filters (polytetrafluoroethylene (PTFE); 0.2 μm, 25 mm) into the cuvettes. Then these were immersed into a toluene bath and allowed to equilibrate for 10 min. At regular time intervals, the scattered light was recorded at an angle of 30 and 45°. The data was collected and processed as far as possible using the ALV-Correlator software, version 3.0.3.2. The CONTIN and cumulant analysis were per-

formed by the software, whereas the double-exponential fits were done manually for the given intensity autocorrelation curves $g_2(t)$. Details can be found in the Supporting Information. Diffusion coefficients and hydrodynamic radii were obtained using the following solvent data: chloroform $n_{20}^{D}=1.44400$, $\eta_{298K}=0.54200$ cp; toluene $n_{20}^{D}=1.49600$, $\eta_{298K}=0.55480$ cp.

Synthesis, materials, and general equipment: Reagents were purchased at reagent grade from commercial sources and used without further purification. All water- and/or air-sensitive reactions were carried out using preheated glassware with standard Schlenk techniques under argon. Unless stated otherwise, all glassware in which the reactions were carried out was evacuated, heated over 100 °C, and flushed with argon prior to loading with the reagents. Solvents were either purchased in anhydrous quality (diethyl ether, diisopropylamine) or were dried and distilled according to standard methods (THF (dried over Na), piperidine (dried over CaH_2), or CH_2Cl_2 (dried over CaH_2)). Solvents used for workup were purified by distillation. ^{1}H and ^{13}C NMR spectra were recorded using a Bruker DPX 300 (^{1}H: 300 MHz, ^{13}C: 75 MHz), DPX 400 (^{1}H: 400 MHz, ^{13}C: 100.6 MHz), or DPX 500 (^{1}H: 500 MHz, ^{13}C: 125.8 MHz) spectrometer. Chemical shifts are given in parts per million (ppm) referenced to residual ^{1}H or ^{13}C signals in deuterated solvents. Mass spectra were measured using a Bruker Daltronics autoflex II TOF/TOF (MALDI-MS; matrix material: DCTB or dithranol), a Finnigan ThermoQuest MAT 95 XL (EI-MS), or an AEI MS-5 (EI-HRMS). Peaks (m/z) smaller than 10% (relative to the basis peak) are not reported. UV/Vis absorption spectra were recorded using a Perkin–Elmer Lambda 18 spectrophotometer using 0.1, 0.2, 1.0, 10, and 100 mm quartz cuvettes manufactured by Hellma. Fluorescence experiments were run on a Perkin–Elmer LS 50 B spectrofluorometer in all-transparent 10 mm quartz cuvettes by monochromatic excitation at the indicated wavelength. Melting points were determined using a Leica DMLB microscope with resistive heating socket controlled using a Leica LMW transformer and a Testo 925 digital thermometer. Thin-layer chromatography (TLC) was conducted on silica-gel-coated aluminum plates (Macherey–Nagel, Alugram SIL G/UV$_{254}$, 0.25 mm coating with fluorescence indicator). For purification by column chromatography silica gel 60M (Macherey–Nagel, 0.04–0.063 mm, 230–400 mesh) was used as the stationary phase that was suspended in the indicated solvent. Gel permeation chromatography (GPC, also size-exclusion chromatography (SEC)) was performed using THF (HPLC grade, stabilized with 2.5 ppm 2,6-di-*tert*-butyl-4-methylphenol (BHT)) at RT. GPC analyses were run using an Agilent Technologies system at a flow rate of 1 mL min^{-1} using an IsoPump G1310A, a G1314B VWD detector, and PSS columns (Polymer Standards Service (PSS), Mainz, Germany; 10^2, 10^3, 10^5, and 10^6 Å; 5 μ; 8×300 mm). All molecular weights were determined after polystyrene (PS) calibration (using PS standard substances obtained from PSS). For the preparative separation of product mixtures by means of GPC, one of two Shimadzu recycling GPC systems was used, equipped with an LC-20 AD pump, an SPD-20A UV detector, and a set of three preparative columns from PSS (either 10^3 Å, 5 μ, 20×300 mm, or linear S, 5 μ, 20×300 mm), operated at a flow rate of 5 mL min^{-1}. GC-MS analysis were performed using a Shimadzu system equipped with an AOC-20i autoinjector, a GCMS-QP2010 Plus mass spectrometer, and a GC-2010 gas chromatograph with an FS-Supreme-5MS column (length 30 m, internal diameter 0.25 mm, film thickness 0.26 μm). The system was operated with helium as carrier gas in the temperature range of 50–340 °C. Microwave-assisted reactions were performed using a Discover Labmate instrument manufactured by CEM.

Here the synthesis of the compounds **7a/b** (by means of the Hart reaction), **9a/b**, **10a/b**, **11a/b**, **12a/b**, **MSW-3a**, **MSW-3b**, **20**, and **22** is described. The synthetic procedures for HPIB, **1**, **2**, **3**, **4**, **5a/b**, **6a/b**, **7a** (by means of amine **3**), **8a/b**, **14**, **15**, **17**, **18**, **20**, **22**, and for some other compounds known from the literature can be found in the Supporting Information.

2′-Iodo-5′-methoxy-4,4″-bis[2-(triisopropylsilyl)ethynyl]-[1,1′:3′,1″]-terphenyl (7a): Iodination: 3,5-Dichloroanisole (2.20 g, 12.43 mmol), [bis-(trifluoroacetoxy)iodo]benzene (2.84 g, 0.52 mmol), and iodine (1.64 g, 0.52 mmol) were dissolved in CH_2Cl_2 (60 mL) and stirred at RT for 2.5 h. The reaction was diluted by the addition of aqueous $NaHSO_3$ (10%) and extracted with CH_2Cl_2. The organic phase was then washed with aqueous $NaHCO_3$ (saturated), water, and brine. After drying over $MgSO_4$ and removal of the solvent, the crude product was purified by column chromatography (petroleum ether (PE)/CH_2Cl_2 25:1, $R_f=0.29$). A white solid was obtained (3.20 g, 85%) that consisted of an inseparable mixture (3:1 w/w) of the desired 2,4-dichloro-3-iodoanisole (2.04 g, 64%) and the undesired 2,4-dichloro-5-iodoanisole (0.80 g, 21%); it was used for the following reaction sequence without further purification. Hart reaction: [2-(4-bromophenyl)ethynyl]triisopropylsilane (see Figure S2 in the Supporting Information) (14.48 g, 42.9 mmol) was dissolved in diethyl ether (50 mL), cooled to −78 °C, and *tert*-butyllithium (1.7 M in pentane; 52.4 mL, 89.1 mmol) was added dropwise. Subsequently, the reaction mixture was stirred for 20 min at this temperature and allowed to warm to 10 °C within 1 h. A solution of the aforementioned iodinated product mixture (2.00 g) in diethyl ether (25 mL) was then added slowly at 10 °C to the intensely colored solution (the colors varied from red to blue among different reactions) of lithiated [2-(4-bromophenyl)ethynyl]triisopropylsilane, then stirred for 15 h at RT. The reaction was quenched by the slow addition of a solution of iodine (16.76 g, 66.0 mmol) in diethyl ether at 0 °C. After stirring for another hour, the reaction mixture was slowly diluted with aqueous $NaHSO_3$ (6%). The layers were separated and the aqueous phase was extracted twice with CH_2Cl_2. The combined organic phases were washed with water and brine. Drying over $MgSO_4$ and removal of the solvent were followed by column chromatography (PE/CH_2Cl_2 1:0 to 9:1). [2-(4-Iodophenyl)ethynyl]triisopropylsilane (8.4 g, colorless liquid) and 2′-iodo-5′-methoxy-4,4″-bis[2-(triisopropylsilyl)ethynyl]-1,1′:3′,1″-terphenyl (2.70 g, 3.6 mmol, yellow solid, 73% (only during the last step), 48% (over the whole reaction sequence)) were isolated. ^{1}H NMR (500 MHz, $CDCl_3$, 298 K): $\delta=7.55$ (d, ^3J(H,H)=8.5 Hz, 4H), 7.31 (d, ^3J(H,H)=8.5 Hz, 4H), 6.82 (s, 2H), 3.81 (s, 3H), 1.15 ppm (br s, 42H); ^{13}C NMR (125 MHz, $CDCl_3$, 298 K): $\delta=159.25$, 148.45, 145.33, 131.79, 129.39, 123.10, 114.93, 106.96, 91.67, 91.41, 55.67, 18.83, 11.47 ppm; MS (EI, 70 eV): m/z calcd for $C_{41}H_{55}IOSi_2$: 746.28; found (%): 746.2 (5) $[M]^+$, 703.1 (10) $[M-C_3H_7]^+$, 544.1 (31) $[M-C_{14}H_{34}]^+$, 501.0 (100) $[M-C_{17}H_{41}]^+$, 473.0 (14) $[M-C_{17}H_{41}Si]^+$, 459.0 (24) $[M-C_{18}H_{42}Si]^+$, 445.0 (25) $[M-C_{19}H_{45}Si]^+$, 431.0 (38) $[M-C_6H_{16}I]^+$.

2′-Iodo-5′-*tert*-butoxy-4,4″-bis[2-(triisopropylsilyl)ethynyl]-[1,1′:3′,1″]-terphenyl (7b): (2-[4-Bromophenyl)ethynyl]triisopropylsilane (see Figure S2 in the Supporting Information) (5.14 g, 13.04 mmol) was dissolved in diethyl ether (10 mL), cooled to −78 °C, and *tert*-butyllithium (1.7 M in pentane; 15.35 mL, 26.09 mmol) added dropwise. Subsequently, the reaction mixture was stirred 20 min at this temperature and allowed to warm to 0 °C within 1 h. Then a solution of 5-*tert*-butoxy-1,3-dichloro-2-iodobenzene (0.50 g, 1.45 mmol) in diethyl ether (10 mL) was added slowly at 0 °C to the colored solution (colors varied from red to blue among different reactions) of lithiated [2-(4-bromophenyl)ethynyl]triisopropylsilane and stirred for 15 h allowing the mixture to warm to RT. The reaction was quenched by the slow addition of iodine (4.05 g, 15.94 mmol) in diethyl ether (30 mL) at 0 °C. After stirring for another two hours, the reaction mixture was slowly diluted with aqueous Na_2SO_3 (6%). The layers were separated, and the aqueous phase was extracted twice with CH_2Cl_2. The combined organic phases were washed with water and brine. Drying over $MgSO_4$ and removal of the solvent were followed by repeated column chromatography (SiO_2, PE/CH_2Cl_2 1:0 to 5:1; Al_2O_3 (Brockmann I+6% H_2O), PE/CH_2Cl_2 96:4). [2-(4-Iodophenyl)ethynyl]triisopropylsilane (4.5 g, colorless liquid) and 2′-iodo-5′-*tert*-butoxy-4,4″-bis[2-(triisopropylsilyl)ethynyl]-1,1′:3′,1″-terphenyl (0.76 g, 66%) were isolated. ^{1}H NMR (300 MHz, $CDCl_3$, 298 K): $\delta=7.59$–7.49 (m, 4H), 7.36–7.27 (m, 4H), 6.90 (s, 2H), 1.37 (s, 9H), 1.15 ppm (s, 42H); ^{13}C NMR (75 MHz, $CDCl_3$, 298 K): $\delta=155.33$, 148.04, 145.24, 131.78, 129.45, 124.34, 123.06, 107.00, 95.16, 91.39, 79.47, 28.97, 18.84, 11.50 ppm; MS (EI, 70 eV): m/z calcd for $C_{44}H_{61}IOSi_2$: 788.33; found (%): 788.4 (10) $[M]^+$, 732.3 (20) $[M-C_4H_8]^+$, 689.3 (100) $[M-C_7H_{15}]$.

Compound 9a: Under Ar, $[Pd(PPh_3)_2Cl_2]$ (28 mg, 39 μmol), CuI (12 mg, 64 μmol), and PPh_3 (32 mg, 0.12 mmol) were suspended in piperidine (15 mL), treated in an ultrasonic bath, and carefully degassed at reduced pressure. Then a solution of **7a** (1.48 g, 1.98 mmol) in THF (3 mL) was added. The mixture was stirred for 15 min, followed by the addition of

8a (2.03 g, 2.78 mmol) dissolved in THF (2 mL). The reaction was immediately placed into a preheated oil bath at 90 °C and heated at reflux for 2 h. Then, to make up for the amount of **8a** that had been lost due to side reactions, an additional amount of **8a** (0.29 g, 0.39 mmol) in THF (2 mL) was added to the red solution. After stirring for another 90 min and cooling to RT, the reaction was diluted with aqueous H_2SO_4 (10%) and CH_2Cl_2. The aqueous phase was extracted another two times with CH_2Cl_2. The combined organic phases were washed with aqueous H_2SO_4 (10%), water, and brine, and then dried over $MgSO_4$. After removal of the solvent under reduced pressure, the crude product was purified by column chromatography (PE/CH_2Cl_2 3:2), and **9a** was obtained as a yellow oil (2.00 g, 75%). ^{1}H NMR (500 MHz, $CDCl_3$, 298 K): δ = 7.62 (d, ^3J(H,H) = 8.2 Hz, 4H), 7.53 (d, ^3J(H,H) = 8.2 Hz, 4H), 6.89 (s, 2H), 6.77 (s, 1H), 6.30 (s, 1H), 3.88 (s, 3H), 3.84 (t, ^3J(H,H) = 6.0 Hz, 2H), 3.75 (t, ^3J(H,H) = 6.7 Hz, 2H), 2.41 (t, ^3J(H,H) = 7.0 Hz, 2H), 1.89–1.78 (m, 2H), 1.78–1.69 (m, 2H), 1.52–1.43 (m, 4H), 1.34–1.18 (m, 48H), 1.14 (br s, 42H), 0.88 (t, ^3J(H,H) = 7.0, 6H), 0.85–0.80 (m, 2H), 0.24 ppm (s, 6H); ^{13}C NMR (125 MHz, $CDCl_3$, 298 K): δ = 159.33, 153.98, 152.62, 146.11, 141.07, 131.66, 129.63, 122.91, 119.86, 117.63, 116.43, 115.33, 114.58, 112.72, 112.47, 107.16, 102.91, 97.48, 94.06, 92.02, 91.33, 69.71, 68.95, 55.67, 32.08, 29.94, 29.91, 29.87, 29.83, 29.75, 29.52, 29.50, 29.00, 26.37, 26.00, 22.85, 20.78, 20.60, 18.86, 15.89, 14.28, 11.50, −1.61 ppm; MS (MALDI-TOF, DCTB): *m/z* calcd for $C_{89}H_{135}NO_3Si_3$: monoisotopic 1349.98, distr. max 1351.29; found: 1349.9 $[M]^+$; GPC (in THF versus PS): M_p = 1713 g mol^{-1}.

Compound 9b: Compound **7b** (420 mg, 532 μmol), **8b** (594 mg, 958 μmol), [$PdCl_2(PPh_3)_2$] (19 mg, 27 μmol), CuI (14 mg, 75 μmol), and PPh_3 (20 mg, 75 μmol) were transferred into a microwave tube. It was evacuated for 1 h and finally refilled with argon. The contents were dissolved in piperidine (3.5 mL) and THF (4.0 mL), and reacted in the microwave (max power 300 W, 120 °C, 12 min). After cooling to RT, the reaction was diluted with aqueous NH_4Cl (saturated) and CH_2Cl_2. The organic phase was washed with aqueous NH_4Cl (saturated), water, and brine, and then dried over $MgSO_4$. After removal of the solvent under reduced pressure, the crude product was purified by column chromatography (PE/EtOAc 24:1), and **9b** was obtained as yellow oil (526 mg, 81%). ^{1}H NMR (400 MHz, CD_2Cl_2, 298 K): δ = 7.69–7.62 (m, 4H), 7.59–7.52 (m, 4H), 7.02 (s, 2H), 6.80 (s, 1H), 6.37 (s, 1H), 3.87 (t, ^3J(H,H) = 6.1 Hz, 2H), 3.78 (t, ^3J(H,H) = 6.7 Hz, 2H), 2.42 (t, ^3J(H,H) = 7.0 Hz, 2H), 1.87–1.70 (m, 4H), 1.56–1.46 (m, 4H), 1.42 (s, 9H), 1.39–1.20 (m, 32H), 1.16 (s, 42H), 0.95–0.79 (m, 8H), 0.28–0.22 ppm (m, 6H); ^{13}C NMR (101 MHz, CD_2Cl_2, 298 K): δ = 156.34, 154.39, 153.19, 145.86, 141.45, 132.02, 130.12, 124.43, 123.30, 120.26, 117.87, 116.95, 115.32, 115.04, 113.34, 107.57, 103.08, 98.24, 94.37, 92.82, 91.86, 80.15, 70.12, 69.54, 32.53, 30.35, 30.31, 30.29, 30.25, 30.13, 29.99, 29.96, 29.93, 29.49, 29.31, 26.79, 26.46, 23.29, 21.24, 20.96, 19.08, 16.22, 14.48, 11.97, −1.53 ppm; MS (MALDI-TOF, DCTB): *m/z* calcd for $C_{84}H_{125}NO_3Si_3$: monoisotopic 1279.90, distr. max: 1281.15; found: 1279.9 $[M]^+$, 1235.1 $[M-C_3H_8]^+$, 1223.8 $[M-C_4H_9]^+$; GPC (in THF versus PS): M_p = 1713 g mol^{-1}.

Compound 10a: Under argon, **9a** (800 mg, 0.59 mmol) and K_2CO_3 (812 mg, 5.92 mmol) were suspended in THF (110 mL) and methanol (45 mL) and stirred for 2 h at RT before the reaction was diluted with water (50 mL) and CH_2Cl_2 (100 mL). After phase separation and extraction of the aqueous layer, the combined organic phases were washed with aqueous H_2SO_4 (10%), water, and brine. After drying over anhydrous $MgSO_4$ and removal of the solvent under reduced pressure, the residue was purified by flash chromatography. Compound **10a** was obtained as a yellow oil (660 mg, 91%). ^{1}H NMR (400 MHz, $CDCl_3$, 298 K): δ = 7.63 (d, ^3J(H,H) = 8.4 Hz, 4H), 7.54 (d, ^3J(H,H) = 8.4 Hz, 4H), 6.90 (s, 2H), 6.82 (s, 1H), 6.33 (s, ^3J(H,H) = 3.8 Hz, 1H), 3.94–3.85 (m, 5H), 3.74 (t, ^3J(H,H) = 6.8 Hz, 2H), 3.28 (s, 1H), 1.80–1.68 (m, 2H), 1.52–1.38 (m, 4H), 1.24 (m, 48H), 1.15 (s, 42H), 0.88 ppm (t, ^3J(H,H) = 6.8 Hz, 6H); ^{13}C NMR (101 MHz, $CDCl_3$, 298 K): δ = 159.35, 153.90, 152.65, 146.13, 141.09, 131.66, 129.63, 122.93, 118.22, 116.74, 115.40, 114.59, 112.76, 111.96, 107.18, 93.92, 91.91, 91.35, 82.03, 80.33, 69.75, 69.27, 55.67, 32.09, 29.87, 29.82, 29.80, 29.64, 29.53, 29.48, 29.23, 28.97, 26.25, 25.99, 22.85, 18.86, 14.27, 11.52 ppm; MS (MALDI-TOF, DCTB): *m/z* calcd for $C_{83}H_{124}O_3Si_2$: monoisotopic 1224.91, distr. max 1226.04); found: 1224.9 $[M]^+$; GPC (in THF versus PS): M_p = 1599 g mol^{-1}.

Compound 10b: Under argon, **10b** (500 mg, 0.43 mmol) and K_2CO_3 (658 mg, 4.76 mmol) were suspended in THF (80 mL) and methanol (32 mL) and stirred for 2 h at RT. Then water and CH_2Cl_2 were added. After phase separation and extraction of the aqueous layer, the combined organic phases were washed with aqueous NH_4Cl (saturated) and brine. Then drying over anhydrous $MgSO_4$, removal of the solvent under reduced pressure, and purification of the residue by column chromatography (SiO_2, PE/CH_2Cl_2 1:1) led to **11b** as a yellow oil (468 mg, 94%). ^{1}H NMR (500 MHz, CD_2Cl_2, 298 K): δ = 7.65 (d, J = 8.5 Hz, 4H), 7.55 (d, J = 8.5 Hz, 4H), 7.03 (s, 2H), 6.85 (s, 1H), 6.38 (s, 1H), 3.89 (t, J = 6.2 Hz, 2H), 3.78 (t, J = 6.8 Hz, 2H), 3.33 (s, 1H), 1.79–1.71 (m, 2H), 1.60–1.43 (m, 4H), 1.42 (s, 9H), 1.26 (m, 34H), 1.16 (s, 42H), 0.91–0.85 ppm (m, 6H); ^{13}C NMR (126 MHz, CD_2Cl_2, 298 K): δ = 156.34, 154.34, 153.16, 145.88, 141.44, 132.03, 130.13, 124.44, 123.30, 118.40, 117.02, 115.40, 115.03, 112.53, 107.55, 94.26, 92.69, 91.86, 82.52, 80.61, 80.15, 70.11, 69.68, 32.53, 30.31, 30.29, 30.28, 30.25, 30.23, 30.05, 29.96, 29.91, 29.73, 29.45, 29.29, 26.67, 26.44, 23.29, 19.06, 14.49, 11.95 ppm; MS (MALDI-TOF, DCTB): *m/z* calcd for $C_{78}H_{114}O_3Si_2$: monoisotopic 1154.83, distr. max 1155.91; found: 1154.8 $[M]^+$, 1110.0 $[M-C_3H_8]^+$, 1098.7 $[M-C_4H_8]^+$; GPC (in THF versus PS): M_p = 1451 g mol^{-1}.

Compound 11a: Compound **10a** (1404 mg, 1.123 mmol) was dissolved in THF and transferred to the reaction flask. After removal of the solvent under reduced pressure [$Pd(PPh_3)_2Cl_2$] (53 mg, 75 μmol), CuI (24 mg, 126 μmol), PPh_3 (53 mg, 201 μmol), hexa(4-iodophenyl)benzene (HPIB; 162 mg, 126 μmol), and piperidine (5 mL) were added. While treating the suspension in an ultrasonic bath, it was degassed by carefully reducing the pressure and refilling the flask with argon repeatedly. The mixture was then immediately immersed into a preheated oil bath and stirred at 80 °C overnight. After cooling to RT, the reaction mixture was diluted with water (40 mL) and CH_2Cl_2. The organic phase was washed successively with aqueous H_2SO_4 (10%), water, and brine, and then dried over $MgSO_4$. The crude product was purified by column chromatography (twice, starting with PE/CH_2Cl_2 = 7:2 up to PE/CH_2Cl_2 = 2:1), and **11a** was obtained as a yellow oil (755 mg, 76%). ^{1}H NMR (500 MHz, $CDCl_3$, 298 K): δ = 7.62 (d, ^3J(H,H) = 8.2 Hz, 24H), 7.52 (d, ^3J(H,H) = 8.2 Hz, 24H), 7.03 (d, ^3J(H,H) = 8.3 Hz, 12H), 6.88 (s, 12H), 6.75 (s, 6H), 6.73 (d, ^3J(H,H) = 8.3 Hz, 12H), 6.28 (s, 6H), 3.87 (s, 18H), 3.83 (t, ^3J(H,H) = 6.0 Hz, 12H), 3.72 (t, ^3J(H,H) = 6.6 Hz, 12H), 1.71 (s, 12H), 1.49–1.39 (m, 24H), 1.33–1.15 (m, 288H), 1.15–1.02 (m, 264H), 0.86 ppm (t, ^3J(H,H) = 6.9 Hz, 36H); ^{13}C NMR (125 MHz, $CDCl_3$, 298 K): δ = 159.17, 153.23, 152.69, 145.98, 141.10, 140.13, 139.95, 131.63, 131.32, 130.47, 129.61, 122.87, 121.03, 117.07, 116.57, 114.55, 114.35, 113.48, 112.91, 107.19, 94.82, 93.65, 92.40, 91.23, 86.55, 69.52, 69.07, 55.63, 32.11, 32.10, 29.97, 29.96, 29.95, 29.90, 29.88, 29.86, 29.84, 29.81, 29.61, 29.57, 29.54, 29.36, 29.01, 26.27, 26.07, 22.87, 22.86, 18.83, 14.29, 11.48 ppm; MS (MALDI-TOF, DCTB): *m/z* calcd for $C_{540}H_{762}O_{18}Si_{12}$: monoisotopic 7871.59, distr. max 7878.84); found: 7877.5 $[M]^+$, 7905.8 $[M+C_2H_4]^+$; GPC (in THF versus PS): M_p = 6550 g mol^{-1}.

Compound 11b: [$PdCl_2(PPh_3)_2$] (14 mg, 20 μmol), CuI (6 mg, 33 μmol), PPh_3 (14 mg, 52 μmol), and hexa(4-iodophenyl)benzene were dissolved in piperidine (5 mL) and degassed by passing Ar through the solution (30 min). At the same time, **10b** (338 mg, 0.293 mmol) was dissolved in THF (1.5 mL) and degassed by passing Ar through the solution (20 min). Finally, the catalyst mixture was heated to 80 °C and the solution of **10b** was added within 10 min. After stirring overnight at 80 °C, the reaction was cooled to RT and diluted with water and CH_2Cl_2. The organic phase was washed successively with aqueous NH_4Cl (saturated), water, and brine, and then dried over $MgSO_4$. The crude product was purified by column chromatography (PE/CH_2Cl_2 2:1 to 1:1) and recycling GPC (SEC) to yield **11b** as a yellow oil (187 mg, 25 μmol, 77%). ^{1}H NMR (400 MHz, CD_2Cl_2, 298 K): δ = 7.62 (d, ^3J(H,H) = 8.4 Hz, 24H), 7.52 (d, ^3J(H,H) = 8.4 Hz, 24H), 7.06 (d, ^3J(H,H) = 8.3 Hz, 12H), 6.99 (s, ^3J-(H,H) = 3.4 Hz, 12H), 6.81 (d, ^3J(H,H) = 8.3 Hz, 12H), 6.77 (s, 6H), 6.31 (s, 6H), 3.84 (t, ^3J(H,H) = 6.0 Hz, 12H), 3.73 (t, ^3J(H,H) = 6.7 Hz, 12H), 1.78–1.65 (m, 12H), 1.50–1.43 (m, 24H), 1.43–1.38 (m, 54H), 1.37–1.16 (m, 192H), 1.16–1.07 (m, 252H), 0.86 ppm (m, 36H); ^{13}C NMR (126 MHz,, 298 K): δ = 155.39, 153.24, 152.79, 145.29, 140.98, 140.12, 140.10, 139.97, 131.62, 131.32, 130.48, 129.65, 124.00, 122.78, 121.02, 117.09, 116.62, 115.02, 114.22, 113.64, 107.21, 94.89, 93.60, 93.00, 91.20,

86.52, 79.66, 69.55, 69.07, 32.14, 32.07, 29.87, 29.84, 29.81, 29.62, 29.60, 29.52, 29.50, 29.39, 29.08, 28.98, 26.30, 26.03, 22.89, 22.84, 18.83, 14.31, 14.28, 11.48 ppm; MS (MALDI-TOF, DCTB): *m/z* calcd for $C_{510}H_{702}O_{18}Si_{12}$: monoisotopic 7451.12, distr. max 7458.05: found: 7457.0 $[M]^+$, 7401.9 $[M-C_4H_9]^+$; GPC (in THF versus PS): $M_p = 6253\ g\,mol^{-1}$.

Compound 12a: Compound **11a** (745 mg, 95 μmol) was dissolved in THF (130 mL) and degassed by ultrasonication under slightly reduced pressure. The solution was cooled to 0 °C, and a solution of TBAF in THF (1 M, 14.2 mL, 14.2 mmol) was added at once. Then the reaction was stirred at room temperature for 3 h and diluted with water. Extraction with CH_2Cl_2 was followed by successive washings with aqueous H_2SO_4 (10%), water, and brine, then drying over $MgSO_4$, and finally removal of the solvent gave the crude product. This was purified by flash chromatography (PE/CH_2Cl_2 30:1) to yield **12a** as a yellow solid (555 mg, 98%). ^{1}H NMR (500 MHz, $CDCl_3$, 298 K): $\delta = 7.62$ (d, ^3J(H,H) = 8.4 Hz, 24H), 7.55 (d, ^3J(H,H) = 8.4 Hz, 24H), 7.02 (d, ^3J(H,H) = 8.4 Hz, 12H), 6.90 (s, 12H), 6.76 (s, 6H), 6.72 (d, ^3J(H,H) = 8.4 Hz, 12H), 6.14 (s, 6H) 3.88 (s, 18H), 3.78 (t, ^3J(H,H) = 6.3 Hz, 12H), 3.71 (t, ^3J(H,H) = 7.1 Hz, 12H), 3.07 (s, 12H), 1.86–1.69 (m, 12H), 1.51–1.41 (m, 24H), 1.38–1.14 (m, 288H), 0.87 ppm (t, ^3J(H,H) = 7.8 Hz, 36H); ^{13}C NMR (125 MHz, $CDCl_3$, 298 K) δ = 159.23, 153.44, 152.56, 145.89, 141.61, 140.11, 139.98, 131.79, 131.34, 130.46, 129.75, 121.41, 120.99, 117.01, 116.34, 114.51, 114.14, 113.39, 113.12, 94.93, 93.70, 92.57, 86.45, 83.73, 77.88, 69.67, 69.14, 55.68, 32.10, 32.09, 29.95, 29.94, 29.93, 29.92, 29.89, 29.86, 29.84, 29.82, 29.57, 29.56, 29.54, 29.48, 29.42, 29.11, 26.16, 25.96, 22.86, 22.86, 14.30, 14.29 ppm; MS (MALDI-TOF, DCTB): *m/z* calcd for $C_{432}H_{522}O_{18}$: monoisotopic 5997.99, distr. max 6002.76; found: 6003.0 $[M]^+$, 6031.8 $[M+C_2H_4]^+$; GPC (in THF versus PS): $M_p = 5922\ g\,mol^{-1}$.

Compound 12b: Compound **11b** (187 mg, 25 μmol) was dissolved in THF (35 mL) and degassed by ultrasonication under reduced pressure. The solution was cooled to 0 °C, and a solution of TBAF in THF (1 M, 6.0 mL, 6.0 mmol) was added at once. The reaction was stirred at room temperature for 3 h and diluted with water. Extraction with CH_2Cl_2 followed by successive washings with aqueous NH_4Cl (saturated), water, and brine, and then drying over $MgSO_4$ prior to removal of the solvent gave the crude product. This was purified by flash chromatography (cyclohexane/CH_2Cl_2 1:1) to yield **12b** as a yellow oil (103 mg, 74%). ^{1}H NMR (500 MHz, CD_2Cl_2) $\delta = 7.67$–7.61 (m, 24H), 7.59–7.52 (m, 24H), 7.06 (d, ^3J(H,H) = 8.5 Hz, 12H), 7.02 (s, 12H), 6.81 (d, ^3J(H,H) = 8.5 Hz, 12H), 6.78 (s, 6H), 6.20 (s, 6H), 3.79 (t, ^3J(H,H) = 6.3 Hz, 12H), 3.73 (t, ^3J(H,H) = 7.0 Hz, 12H), 3.14 (s, 12H), 1.80–1.70 (m, 12H), 1.52–1.44 (m, 24H), 1.43–1.40 (m, 54H), 1.37–1.16 (m, 204H), 0.86 ppm (m, 36H); ^{13}C NMR (101 MHz, CD_2Cl_2, 298 K) $\delta = 156.22$, 153.89, 153.13, 145.66, 141.95, 140.69, 140.54, 132.19, 131.93, 130.70, 130.22, 124.39, 121.80, 121.44, 117.36, 116.80, 115.41, 114.41, 113.89, 95.13, 94.08, 93.35, 86.89, 83.98, 80.15, 78.28, 70.10, 69.67, 32.57, 32.51, 30.33, 30.31, 30.27, 30.24, 30.23, 30.20, 30.02, 30.00, 29.95, 29.91, 29.87, 29.54, 29.29, 26.65, 26.36, 23.33, 23.28, 14.53, 14.48 ppm; MS (MALDI-TOF, DCTB): *m/z* calcd for $C_{402}H_{462}O_{18}$: monoisotopic 5577.52, distr max 5581.96; found: 5582.0 $[M]^+$; GPC (in THF versus PS): $M_p = 5622\ g\,mol^{-1}$.

Compound MSW-3a: Compound **12a** (200 mg, 33.3 μmol) was dissolved in THF (25 mL) and added with a constant rate over 90 h to a solution of $[Pd(PPh_3)_2Cl_2]$ (28 mg, 40 μmol), CuI (12 mg, 62 μmol), and iodine (56 mg, 220 μmol) in THF (50 mL) and diisopropyl amine (60 mL) at 50 °C. After the addition was completed, the syringe was refilled trice with THF (7 mL), and the solutions were added over 90 min to the catalyst system. The reaction was cooled to RT and diluted with water (200 mL) and CH_2Cl_2. The organic phase was washed successively with aqueous H_2SO_4 (10%), aqueous $NaHSO_3$ (10%), water, and brine, and then dried over $MgSO_4$. After removal of the solvent, the crude product was filtered over SiO_2 (PE/CH_2Cl_2 1:4) and purified by recycling GPC by using THF as eluent. To remove BHT, the vials that contained the product were combined, the solvent removed, and the product precipitated from CH_2Cl_2 and methanol. After filtration, **MSW-3a** was obtained as a yellow solid (158 mg, 79%). ^{1}H NMR (500 MHz, $CDCl_3$, 298 K): $\delta = 7.68$ (d, ^3J(H,H) = 8.4 Hz, 24H), 7.58 (d, ^3J(H,H) = 8.4 Hz, 24H), 7.08 (d, ^3J(H,H) = 8.3 Hz, 12H), 6.96 (s, 12H), 6.84 (s, 6H), 6.74 (d, ^3J(H,H) = 8.3 Hz, 12H), 6.44 (s, 6H), 3.91 (s, 18H), 3.87 (t, ^3J(H,H) = 6.6 Hz, 12H), 3.75 (t, ^3J(H,H) = 7.0 Hz, 12H), 1.82–1.74 (m, 12H), 1.54–1.42 (m, 24H), 1.40–1.03 (m, 300H), 0.86 (t, ^3J(H,H) = 7.0 Hz, 18H), 0.85 ppm (t, ^3J(H,H) = 7.0 Hz, 18H); ^{13}C NMR (125 MHz, $CDCl_3$, 298 K): $\delta = 159.39$, 153.12, 153.02, 145.75, 141.87, 140.06, 139.98, 132.12, 131.34, 130.65, 129.96, 121.16, 120.75, 117.43, 116.38, 114.45, 114.04, 113.59, 113.16, 94.56, 92.95, 92.12, 86.22, 81.63, 74.69, 69.63, 69.51, 55.71, 32.09, 29.96, 29.91, 29.89, 29.85, 29.84, 29.79, 29.67, 29.65, 29.55, 29.35, 29.14, 26.12, 26.05, 22.86, 14.29 ppm; MS (MALDI-TOF, DCTB): *m/z* calcd for $C_{432}H_{510}O_{18}$, monoisotopic 5985.90, distr max 5990.66: found: 5990.7 $[M]^+$, 6018.5 $[M+C_2H_4]^+$; GPC (in THF versus PS): $M_p = 5555\ g\,mol^{-1}$.

Compound MSW-3b: CuI (6.5 mg, 33.9 μmol) and iodine (22.0 mg, 96.8 μmol) were dissolved in THF (75 mL) and diisopropyl amine (70 mL). This solution was saturated with air by bubbling it through the solution for 1 h. Then $[Pd(PPh_3)_2Cl_2]$ (13.6 mg, 19 μmol) was added, and the solution heated to 50 °C. Under vigorous stirring, a solution of **12b** (27.0 mg, 4.84 μmol) in THF (30 mL) was added with a constant rate over 48 h to the catalyst solution held at 50 °C. The reaction was diluted with water and CH_2Cl_2, and the organic phase was washed successively with aqueous NH_4Cl (saturated), aqueous Na_2SO_3 (10%), and brine, and then dried over $MgSO_4$. After removal of the solvent, the crude product was purified by column chromatography (SiO_2, cyclohexane/CH_2Cl_2 12:11) and recycling GPC (SEC) by using THF as eluent. To remove BHT, the vials that contained the product were combined, the solvent removed, and the product precipitated from CH_2Cl_2 and methanol. After filtration, **MSW-3b** was obtained as a yellow solid (18.0 mg, 68%). ^{1}H NMR (500 MHz, 298 K): $\delta = 7.70$ (d, ^3J(H,H) = 8.4 Hz, 24H), 7.61 (d, ^3J(H,H) = 8.5 Hz, 24H), 7.11 (d, ^3J(H,H) = 8.4 Hz, 12H), 7.08 (s, 12H), 6.88–6.83 (m, 18H), 6.48 (s, 6H), 3.89 (t, ^3J(H,H) = 6.7 Hz, 12H), 3.78 (t, ^3J(H,H) = 7.1 Hz, 12H), 1.82–1.73 (m, 12H), 1.51–1.45 (m, 12H), 1.44 (s, 54H), 1.38–1.13 (m, 216H), 0.83 ppm (m, 36H); ^{13}C NMR (126 MHz, 298 K): $\delta = 156.32$, 153.52, 153.41, 145.54, 142.28, 140.76, 140.37, 132.53, 131.94, 130.73, 130.43, 124.40, 121.38, 121.27, 117.74, 116.69, 115.51, 114.20, 113.89, 94.65, 93.41, 92.89, 86.83, 81.97, 80.23, 74.92, 70.01, 69.89, 32.57, 32.50, 30.37, 30.34, 30.30, 30.28, 30.24, 30.12, 30.08, 30.01, 29.98, 29.80, 29.55, 29.27, 26.59, 26.46, 23.28, 14.50, 14.46 ppm; MS (MALDI-TOF, DCTB): *m/z* calcd for $C_{402}H_{450}O_{18}$: monoisotopic 5565.43, distr max 5569.86; found: 5569.9 $[M]^+$, 5513.2 $[M-C_4H_8]^+$; GPC (in THF versus PS): $M_p = 5289\ g\,mol^{-1}$.

Compound 20: 4-Iodo-1,1′-biphenyl (32.9 mg, 0.118 mmol), CuI (2.6 mg, 0.014 mmol), $[Pd_2(dba)_3]$ (4.1 mg, 0.005 mmol), and (diphenylphosphino)-ferrocene (dppf; 4.9 mg, 0.009 mmol) were dissolved in THF (2 mL) and piperidine (5 mL) in a microwave tube. After sealing the tube and purging the solution for 30 min with argon, compound **18** (80.0 mg, 0.112 mmol) was added, and the mixture was heated under microwave irradiation (120 °C, 12 min, max power 300 W). The reaction was diluted with CH_2Cl_2 and washed with aqueous H_2SO_4 (10%), water, and brine, and then dried over $MgSO_4$. Filtration and removal of the solvent followed by column chromatography (cyclohexane/CH_2Cl_2 5:1) and recrystallization from ethanol yielded **20** as a yellow solid (74.6 mg, 0.086 mmol, 77%). M.p. 78 °C; ^{1}H NMR (400 MHz, CD_2Cl_2, 298 K): δ = 7.69–7.57 (m, 6H), 7.53–7.43 (m, 4H), 7.38 (m, 1H), 7.04 (s, 1H), 7.02 (s, 1H), 6.95–6.87 (m, 2H), 4.04 (m, 4H), 3.83 (s, 3H), 1.92–1.79 (m, 4H), 1.62–1.50 (m, 4H), 1.45–1.19 (m, 48H), 0.87 ppm (m, 6H); MS (EI, 70 eV): *m/z* calcd for $C_{61}H_{84}O_3$: 865.32: found (%): 864.6 (100) $[M]^+$, 640.4 (10) $[M-C_{16}H_{32}]^+$, 429.1 (20) $[M-C_{31}H_{63}]^+$, 401.1 (20) $[M-C_{33}H_{67}]^+$; 387.1 (12) $[M-C_{33}H_{67}O]^+$.

Compound 22: 4,4″-Diiodo-*p*-terphenyl (11.0 mg, 22.8 μmol), CuI (0.5 mg, 2.5 μmol), $[Pd(PPh_3)_2Cl_2]$ (1.0 mg, 1.4 μmol), and PPh_3 (1.2 mg, 4.6 μmol) were dissolved in THF (1 mL) and piperidine (4 mL) in a microwave tube. Compound **18** (34.2 mg, 47.9 μmol) was added and the mixture was heated under microwave irradiation (120 °C, 12 min, max power 300 W). After cooling to RT, the reaction was diluted with methyl *tert*-butyl ether (MTBE) and CH_2Cl_2, and washed with aqueous H_2SO_4 (10%), water, and brine, followed by drying over $MgSO_4$. Filtration and removal of the solvent followed by column chromatography (cyclohexane/CH_2Cl_2 2:1) gave a crude product. Further purification involved recrystallization from hot chloroform and methanol and recycling GPC (SEC) of the solid. Compound **22** (27 mg, 16.3 μmol, 72%) was obtained

as a yellow solid. ^{1}H NMR (400 MHz, $CDCl_3$, 298 K): $\delta = 7.71$ (s, 4H), 7.68–7.59 (m, 8H), 7.51–7.45 (m, 4H), 7.03 (s, 2H), 7.01 (s, 2H), 6.93–6.85 (m, 4H), 4.04 (m, 8H), 3.84 (s, 6H), 1.92–1.80 (m, 8H), 1.64–1.49 (m, 8H), 1.47–1.17 (m, 96H), 0.93–0.83 ppm (m, 12H); ^{13}C NMR (101 MHz, $CDCl_3$, 298 K): $\delta = 159.82$, 153.89, 153.66, 140.31, 139.71, 133.21, 132.21, 127.56, 126.97, 122.80, 117.15, 117.01, 115.78, 114.67, 114.13, 113.71, 95.18, 94.77, 87.14, 84.84, 69.85, 69.82, 55.44, 32.08, 29.88, 29.87, 29.84, 29.82, 29.80, 29.62, 29.62, 29.55, 29.52, 26.28, 26.25, 22.84, 14.27 ppm; MS (MALDI-TOF, DCTB): *m*/*z* calcd for $C_{116}H_{162}O_6$: monoisotopic 1651.24, distr max 1652.52); found: 1651.2 $[M]^+$.

Acknowledgements

This work was financially supported by the Deutsche Forschungsgemeinschaft (DFG), the Sonderforschungsbereich (SFB) 624, and the Fonds der Chemischen Industrie (FCI).

[1] a) J. S. Moore, J. S. Zhang, *Angew. Chem.* **1992**, *104*, 873–874; *Angew. Chem. Int. Ed. Engl.* **1992**, *31*, 922–924; b) F. Diederich, *Nature* **1994**, *369*, 199–207; c) M. M. Haley, *Synlett* **1998**, 557–565; d) Q. Zhou, P. J. Carroll, T. M. Swager, *J. Org. Chem.* **1994**, *59*, 1294–1301; e) H. A. Staab, K. Neunhoeffer, *Synthesis* **1974**, 424–424; f) G. Eglinton, A. R. Galbraith, *Proc. Chem. Soc.* **1957**, 350–351; g) O. M. Behr, G. Eglinton, A. R. Galbraith, R. A. Raphael, *J. Chem. Soc.* **1960**, 3614–3625; h) E. L. Spitler, C. A. Johnson, M. M. Haley, *Chem. Rev.* **2006**, *106*, 5344–5386; i) H. A. Staab, F. Graf, *Tetrahedron Lett.* **1966**, *7*, 751–757; j) H. A. Staab, J. Ipaktschi, A. Nissen, *Chem. Ber. Recl.* **1971**, *104*, 1182–1190; k) I. D. Campbell, G. Eglinton, W. Henderson, R. A. Raphael, *J. Chem. Soc. Chem. Commun.* **1966**, 87–89; l) M. Nakagawa, *Pure Appl. Chem.* **1975**, *44*, 885–924; m) M. Nakagawa, *Angew. Chem.* **1979**, *91*, 215–226; *Angew. Chem. Int. Ed. Engl.* **1979**, *18*, 202–214; n) H. N. C. Wong, P. J. Garratt, F. Sondheimer, *J. Am. Chem. Soc.* **1974**, *96*, 5604–5605; o) F. Sondheimer, *Acc. Chem. Res.* **1972**, *5*, 81–91.

[2] a) W. Zhang, J. S. Moore, *Angew. Chem.* **2006**, *118*, 4524–4548; *Angew. Chem. Int. Ed.* **2006**, *45*, 4416–4439; b) J. Sakamoto, J. van Heijst, O. Lukin, A. D. Schlüter, *Angew. Chem.* **2009**, *121*, 1048–1089; *Angew. Chem. Int. Ed.* **2009**, *48*, 1030–1069; c) J. S. Moore, *Acc. Chem. Res.* **1997**, *30*, 402–413; d) U. H. F. Bunz, Y. Rubin, Y. Tobe, *Chem. Soc. Rev.* **1999**, *28*, 107–119; e) W. B. Wan, M. M. Haley, *J. Org. Chem.* **2001**, *66*, 3893–3901; f) T. Yoshimura, A. Inaba, M. Sonoda, K. Tahara, Y. Tobe, R. V. Williams, *Org. Lett.* **2006**, *8*, 2933–2936; g) W. B. Wan, S. C. Brand, J. J. Pak, M. M. Haley, *Chem. Eur. J.* **2000**, *6*, 2044–2052; h) M. M. Haley, S. C. Brand, J. J. Pak, *Angew. Chem.* **1997**, *109*, 863–866; *Angew. Chem. Int. Ed. Engl.* **1997**, *36*, 836–838; i) I. Hisaki, M. Sonoda, Y. Tobe, *Eur. J. Org. Chem.* **2006**, 833–847; j) S. Höger, *J. Polym. Sci. Part A* **1999**, *37*, 2685–2698; k) S. Höger, A. D. Meckenstock, *Chem. Eur. J.* **1999**, *5*, 1686–1691.

[3] J. Zhang, D. J. Pesak, J. L. Ludwick, J. S. Moore, *J. Am. Chem. Soc.* **1994**, *116*, 4227–4239.

[4] C. Grave, A. D. Schlüter, *Eur. J. Org. Chem.* **2002**, 3075–3098.

[5] a) M. E. Gallina, C. Giansante, P. Ceroni, M. Venturi, J. Sakamoto, A. D. Schlüter, *Eur. J. Inorg. Chem.* **2011**, 1479–1486; b) K. Becker, P. G. Lagoudakis, G. Gaefke, S. Höger, J. M. Lupton, *Angew. Chem.* **2007**, *119*, 3520–3525; *Angew. Chem. Int. Ed.* **2007**, *46*, 3450–3455; c) A. D. Slepkov, F. A. Hegmann, R. R. Tykwinski, K. Kamada, K. Ohta, J. A. Marsden, E. L. Spitler, J. J. Miller, M. M. Haley, *Opt. Lett.* **2006**, *31*, 3315–3317; d) K. Ohta, S. Yamada, K. Kamada, A. D. Slepkov, F. A. Hegmann, R. R. Tykwinski, L. D. Shirtcliff, M. M. Haley, P. Salek, F. Gel′mukhanov, H. Agren, *J. Phys. Chem. A* **2011**, *115*, 105–117; e) E. L. Spitler, J. M. Monson, M. M. Haley, *J. Org. Chem.* **2008**, *73*, 2211–2223; f) A. Sarkar, J. J. Pak, G. W. Rayfield, M. M. Haley, *J. Mater. Chem.* **2001**, *11*, 2943–2945; g) T. Naddo, Y. Che, W. Zhang, K. Balakrishnan, X. Yang, M. Yen, J. Zhao, J. S. Moore, L. Zang, *J. Am. Chem. Soc.* **2007**, *129*, 6978–6979; h) M. Fritzsche, A. Bohle, D. Dudenko, U. Baumeister, D. Sebastiani, G. Richardt, H. W. Spiess, M. R. Hansen, S. Höger, *Angew. Chem.* **2011**, *123*, 3086–3089; *Angew. Chem. Int. Ed.* **2011**, *50*, 3030–3033; i) S. Höger, X. H. Cheng, A. D. Ramminger, V. Enkelmann, A. Rapp, M. Mondeshki, I. Schnell, *Angew. Chem.* **2005**, *117*, 2862–2866; *Angew. Chem. Int. Ed.* **2005**, *44*, 2801–2805; j) S. Höger, V. Enkelmann, K. Bonrad, C. Tschierske, *Angew. Chem.* **2000**, *112*, 2356–2358; *Angew. Chem. Int. Ed.* **2000**, *39*, 2268–2270; k) S. Höger, *Chem. Eur. J.* **2004**, *10*, 1320–1329; l) O. Y. Mindyuk, M. R. Stetzer, P. A. Heiney, J. C. Nelson, J. S. Moore, *Adv. Mater.* **1998**, *10*, 1363–1366; m) S. H. Seo, T. V. Jones, H. Seyler, J. O. Peters, T. H. Kim, J. Y. Chang, G. N. Tew, *J. Am. Chem. Soc.* **2006**, *128*, 9264–9265.

[6] a) S. Höger, K. Becker, G. Gaefke, J. Rolffs, J. M. Lupton, *Chem. Commun.* **2010**, 4686–4688; b) J. Luo, Q. Yan, Y. Zhou, T. Li, N. Zhu, C. Bai, Y. Cao, J. Wang, J. Pei, D. Zhao, *Chem. Commun.* **2010**, *46*, 5725–5727.

[7] S. Dawn, M. B. Dewal, D. Sobransingh, M. C. Paderes, A. C. Wibowo, M. D. Smith, J. A. Krause, P. J. Pellechia, L. S. Shimizu, *J. Am. Chem. Soc.* **2011**, *133*, 7025–7032.

[8] a) S. Furukawa, K. Tahara, F. C. De Schryver, M. Van der Auweraer, Y. Tobe, S. De Feyter, *Angew. Chem.* **2007**, *119*, 2889–2892; *Angew. Chem. Int. Ed.* **2007**, *46*, 2831–2834; b) S. Furukawa, H. Uji-i, K. Tahara, T. Ichikawa, M. Sonoda, F. C. De Schryver, Y. Tobe, S. De Feyter, *J. Am. Chem. Soc.* **2006**, *128*, 3502–3503; c) S. B. Lei, K. Tahara, F. C. De Schryver, M. Van der Auweraer, Y. Tobe, S. De Feyter, *Angew. Chem.* **2008**, *120*, 3006–3010; *Angew. Chem. Int. Ed.* **2008**, *47*, 2964–2968; d) J. Adisoejoso, K. Tahara, S. Okuhata, S. Lei, Y. Tobe, S. De Feyter, *Angew. Chem.* **2009**, *121*, 7489–7493; *Angew. Chem. Int. Ed.* **2009**, *48*, 7353–7357; e) K. Tahara, S. Okuhata, J. Adisoejoso, S. B. Lei, T. Fujita, S. De Feyter, Y. Tobe, *J. Am. Chem. Soc.* **2009**, *131*, 17583–17590; f) K. Tahara, S. B. Lei, J. Adisoejoso, S. De Feyter, Y. Tobe, *Chem. Commun.* **2010**, *46*, 8507–8525; g) S.-S. Jester, D. Schmitz, F. Eberhagen, S. Höger, *Chem. Commun.* **2011**, *47*, 8838–8840; h) S.-S. Jester, E. Sigmund, S. Höger, *J. Am. Chem. Soc.* **2011**, *133*, 11062–11065; i) S.-S. Jester, N. Shabelina, S. M. Le Blanc, S. Höger, *Angew. Chem.* **2010**, *122*, 6237–6241; *Angew. Chem. Int. Ed.* **2010**, *49*, 6101–6105; j) J. A. A. W. Elemans, S. B. Lei, S. De Feyter, *Angew. Chem.* **2009**, *121*, 7434–7469; *Angew. Chem. Int. Ed.* **2009**, *48*, 7298–7332; k) T. Chen, G.-B. Pan, H. Wettach, M. Fritzsche, S. Höger, L. J. Wan, H. B. Yang, B. H. Northrop, P. J. Stang, *J. Am. Chem. Soc.* **2010**, *132*, 1328–1333; l) G.-B. Pan, X. H. Cheng, S. Höger, W. Freyland, *J. Am. Chem. Soc.* **2006**, *128*, 4218–4219.

[9] a) J. A. Marsden, J. J. Miller, M. M. Haley, *Angew. Chem.* **2004**, *116*, 1726–1729; *Angew. Chem. Int. Ed.* **2004**, *43*, 1694–1697; b) W. Zhang, J. S. Moore, *J. Am. Chem. Soc.* **2005**, *127*, 11863–11870; c) W. Zhang, J. S. Moore, *J. Am. Chem. Soc.* **2004**, *126*, 12796–12796; d) D. E. Gross, J. S. Moore, *Macromolecules* **2011**, *44*, 3685–3687; e) A. J. Gallant, M. J. MacLachlan, *Angew. Chem.* **2003**, *115*, 5465–5468; *Angew. Chem. Int. Ed.* **2003**, *42*, 5307–5310; f) I. Hisaki, Y. Sakamoto, H. Shigemitsu, N. Tohnai, M. Miyata, S. Seki, A. Saeki, S. Tagawa, *Chem. Eur. J.* **2008**, *14*, 4178–4187.

[10] a) D. Mössinger, D. Chaudhuri, T. Kudernac, S. Lei, S. De Feyter, J. M. Lupton, S. Höger, *J. Am. Chem. Soc.* **2010**, *132*, 1410–1423; b) S. Lei, A. Ver Heyen, S. De Feyter, M. Surin, R. Lazzaroni, S. Rosenfeldt, M. Ballauff, P. Lindner, D. Mössinger, S. Höger, *Chem. Eur. J.* **2009**, *15*, 2518–2535; c) D. Mössinger, J. Hornung, S. Lei, S. De Feyter, S. Höger, *Angew. Chem.* **2007**, *119*, 6926–6930; *Angew. Chem. Int. Ed.* **2007**, *46*, 6802–6806.

[11] a) T. C. Bedard, J. S. Moore, *J. Am. Chem. Soc.* **1995**, *117*, 10662–10671; b) J. A. Marsden, M. J. O'Connor, M. M. Haley, *Org. Lett.* **2004**, *6*, 2385–2388; c) M. Laskoski, W. Steffen, J. G. M. Morton, M. D. Smith, U. H. F. Bunz, *J. Organomet. Chem.* **2003**, *673*, 25–39; d) T. Takeda, A. G. Fix, M. M. Haley, *Org. Lett.* **2010**, *12*, 3824–3827.

[12] a) S. H. Jung, W. Pisula, A. Rouhanipour, H. J. Räder, J. Jacob, K. Müllen, *Angew. Chem.* **2006**, *118*, 4801–4806; *Angew. Chem. Int. Ed.* **2006**, *45*, 4685–4690; b) S. Höger, A. D. Meckenstock, H.

Pellen, *J. Org. Chem.* **1997**, *62*, 4556–4557; c) A. Ziegler, W. Mamdouh, A. Ver Heyen, M. Surin, H. Uji, M. M. S. Abdel-Mottaleb, F. C. De Schryver, S. De Feyter, R. Lazzaroni, S. Höger, *Chem. Mater.* **2005**, *17*, 5670–5683.

[13] a) S. Anderson, H. L. Anderson, J. K. M. Sanders, *Acc. Chem. Res.* **1993**, *26*, 469–475; b) D. H. Busch, *Top. Curr. Chem. Vol. 249* (Eds.: C. A. Schalley, F. Vögtle, K. H. Dötz), Springer Berlin/Heidelberg, **2005**, 1–65; c) Z. R. Laughrey, B. C. Gibb, *Top. Curr. Chem. Vol. 249* (Eds.: C. A. Schalley, F. Vögtle, K. H. Dötz), Springer Berlin/Heidelberg, **2005**, 67–125; d) J. K. Sprafke, D. V. Kondratuk, M. Wykes, A. L. Thompson, M. Hoffmann, R. Drevinskas, W.-H. Chen, C. K. Yong, J. Kärnbratt, J. E. Bullock, M. Malfois, M. R. Wasielewski, B. Albinsson, L. M. Herz, D. Zigmantas, D. Beljonne, H. L. Anderson, *J. Am. Chem. Soc.* **2011**, *133*, 17262–17273; e) M. C. O'Sullivan, J. K. Sprafke, D. V. Kondratuk, C. Rinfray, T. D. W. Claridge, A. Saywell, M. O. Blunt, J. N. O'Shea, P. H. Beton, M. Malfois, H. L. Anderson, *Nature* **2011**, *469*, 72–75.

[14] S. Höger, V. Enkelmann, *Angew. Chem.* **1996**, *107*, 2917–2919; *Angew. Chem. Int. Ed. Engl.* **1995**, *34*, 2713–2716.

[15] a) U. H. F. Bunz, *Chem. Rev.* **2000**, *100*, 1605–1644; b) P. M. Cotts, T. M. Swager, Q. Zhou, *Macromolecules* **1996**, *29*, 7323–7328; c) A. Godt, M. Schulte, H. Zimmermann, G. Jeschke, *Angew. Chem.* **2006**, *118*, 7722–7726; *Angew. Chem. Int. Ed.* **2006**, *45*, 7560–7564.

[16] Acyclic alternating rigid rod/corner copolymers behave as freely rotating chains (in which the degrees of freedom of the corner segments are restricted to rotational motion of the rod units). Note: Freely jointed chains consist of rigid rod units that are connected by flexible linker units. On the contrary, in freely rotating chains the rigid rods are linked by corner units that allow a rotation.

[17] a) C. Grave, A. D. Schlüter, *Eur. J. Org. Chem.* **2002**, 3075–3098; b) M. Xanthos, *Functional Fillers for Plastics*, VCH, Weinheim, **2005**.

[18] M. Albrecht, Yeni, R. Fröhlich, *Synlett* **2007**, 2295–2297.

[19] a) W. B. Smith, O. C. Ho, *J. Org. Chem.* **1990**, *55*, 2543–2545; b) L. Malet-Sanz, J. Madrzak, R. S. Holvey, T. Underwood, *Tetrahedron Lett.* **2009**, *50*, 7263–7267.

[20] a) C. J. F. Du, H. Hart, K. K. D. Ng, *J. Org. Chem.* **1986**, *51*, 3162–3165; b) A. Saednya, H. Hart, *Synthesis* **1996**, 1455.

[21] Direct conversion of **5a** to **7a** fails due to a strong *ortho*-directing effect of the methoxy substituent. While Hart et al. were able to obtain the terphenyl directly from 1,3-dichlorobenzene and the lithiumorganyl, the reaction of **5a** with 4-[2-(triisopropylsilyl)ethynyl]-phenyl lithium (formed from 1-bromo-4-(triisopropylsilylethynyl)-benzene and *t*BuLi) leads to 5-chloro-2-iodo-3-methoxy-4′-[2-(triisopropylsilyl)ethynyl]biphenyl; a) S. Höger, *Liebigs Ann. Recl.* **1997**, 273–277; b) N. J. R. van Eikema Hommes, P. von Ragué Schleyer, *Angew. Chem.* **1992**, *104*, 768–771; *Angew. Chem. Int. Ed. Engl.* **1992**, *31*, 755–758; c) F. M. Irvine, J. C. Smith, *J. Chem. Soc.* **1927**, 74–77.

[22] Iodination with *N*-iodosuccinimide (NIS) (product ratio: 3:1, overall yield <50%), iodic acid, and iodine (product ratio 1:1), and bis(*tert*-butylcarbonyloxy)iodobenzene or bis(acetoxy)iodobenzene (no reaction) were inferior. A more regioselective iodination method that gave a ratio of 16:1 was reported after completion of this work by Lehmler et al.: S. N. Joshi, S. M. Vyas, H. Wu, M. W. Duffel, S. Parkin, H.-J. Lehmler, *Tetrahedron* **2011**, *67*, 7461–7469.

[23] A. Godt, O. Ünsal, M. Roos, *J. Org. Chem.* **2000**, *65*, 2837–2842.

[24] This was ascribed to an artificially increased ratio between the lithium organyl and **6a** (as opposed to adding **6a** all at once).

[25] H. Hart, K. Harada, C. J. F. Du, *J. Org. Chem.* **1985**, *50*, 3104–3110.

[26] C. Elschenbroich, *Organometallchemie*, 5th ed., Teubner, Wiesbaden, 2 **005**.

[27] Starting with commercially available compounds, the Suzuki coupling affords a five-step synthesis, whereas the Hart reaction requires only three. This includes the preparation of the lithiated compound for the latter and the preparation of the boronic ester for the former reaction.

[28] J. L. Holcombe, T. Livinghouse, *J. Org. Chem.* **1986**, *51*, 111–113.

[29] The deprotonation of 3,5-dichloranisole in THF at −78°C with *t*BuLi (1.2 equiv) followed by the addition of iodine in THF led to a product mixture of unreacted 3,5-dichloroanisole (34%), 3,5-dichloro-2-iodoanisole (38%), and 3,5-dichloro-2,6-diiodoanisole (21%) along with some unknown side products (7%). These ratios were determined by GC-MS.

[30] a) M. Iwao, *J. Org. Chem.* **1990**, *55*, 3622–3627; b) F. Toudic, A. Turck, N. Ple, G. Queguiner, M. Darabantu, T. Lequeux, J. C. Pommelet, *J. Heterocycl. Chem.* **2003**, *40*, 855–860.

[31] a) M. J. Plater, J. P. Sinclair, S. Aiken, T. Gelbrich, M. B. Hursthouse, *Tetrahedron* **2004**, *60*, 6385–6394; b) W. A. Daoud, M. L. Turner, *Bull. Chem. Soc. Jpn.* **2005**, *78*, 367–369; c) N. González-Rojano, E. Arias-Marín, D. Navarro-Rodríguez, S. Weidner, *Synlett* **2005**, 1259–1262; d) C. S. Andersen, K. V. Gothelf, *Org. Biomol. Chem.* **2009**, *7*, 58–60; e) J.-F. Morin, T. Sasaki, Y. Shirai, J. M. Guerrero, J. M. Tour, *J. Org. Chem.* **2007**, *72*, 9481–9490; f) K. Kobayashi, N. Kobayashi, M. Ikuta, B. Therrien, S. Sakamoto, K. Yamaguchi, *J. Org. Chem.* **2005**, *70*, 749–752.

[32] R. Chinchilla, C. Nájera, *Chem. Soc. Rev.* **2011**, *40*, 5084–5121.

[33] Partially deprotected **7a** was isolated in a yield of 20%.

[34] T. Hundertmark, A. F. Littke, S. L. Buchwald, G. C. Fu, *Org. Lett.* **2000**, *2*, 1729–1731.

[35] The system was reported without DBU and with dioxane as solvent and diisopropyl amine as base. Heating was not required and reaction times were between 0.5 and 15 h. In the present case, this system did not give any product, even at 80°C (conventional heating) or after 12 min of microwave irradiation at 120°C. Only the starting material was observed by TLC.

[36] A. Soheili, J. Albaneze-Walker, J. A. Murry, P. G. Dormer, D. L. Hughes, *Org. Lett.* **2003**, *5*, 4191–4194.

[37] a) C. Oliver Kappe, *Chem. Soc. Rev.* **2008**, *37*, 1127–1139; b) V. P. Mehta, E. V. Van der Eycken, *Chem. Soc. Rev.* **2011**, *40*, 4925–4936.

[38] a) G. Gaefke, S. Höger, *Synthesis* **2008**, 2155–2157; b) S. Höger, K. Bonrad, *J. Org. Chem.* **2000**, *65*, 2243–2245.

[39] Most likely the lower yield of the cyclization of **12b** can be ascribed to the smaller scale on which the reaction was performed (relative to **12a**).

[40] For the addition all at once (0 h; within 1 min), the concentration of **12a** in the receiver is calculated directly by dividing the amount of **12a** in the syringe by the total volume. All other concentrations were calculated by assuming a drop size of 0.05 mL of the solution of **12a** in THF. The average concentration of **12a** in the receiver, after addition of a drop, was calculated according to the following equation: c(**12a** in receiver) = [c(**12a** in syringe) × 0.05 mLV^{-1}-(receiver) + c(**12a** in syringe) × 0.05 mL/[V(receiver) + V(syringe)]]/2 (= average concentration of **12a** in the receiver, by considering the first and the last drop that is added). We assume in this calculation that all bisacetylene of one drop is completely coupled before the next drop reaches the solution.

[41] Assuming the dimer to have an extinction coefficient that is twice as large as for the monomer, the amount of dimer was reduced from approximately 3% to approximately 1%.

[42] D. Mössinger, S.-S. Jester, E. Sigmund, U. Müller, S. Höger, *Macromolecules* **2009**, *42*, 7974–7978.

[43] a) A. M. Boldi, F. Diederich, *Angew. Chem.* **1994**, *106*, 482–485; *Angew. Chem. Int. Ed. Engl.* **1994**, *33*, 468–471; b) Y. Pang, J. Li, B. Hu, F. E. Karasz, *Macromolecules* **1999**, *32*, 3946–3950; c) L. Liao, Y. Pang, L. M. Ding, F. E. Karasz, *J. Polym. Sci. Part A* **2003**, *41*, 3149–3158; d) S. Amiri, P. R. Schreiner, *J. Phys. Chem. A* **2009**, *113*, 11750–11757.

[44] Since absorption and emission of **MSW-3a** and **MSW-3b** are nearly identical (see the Supporting Information), we currently do not believe that the formation of hydrogen aggregates can be responsible for alterations of such a large extent.

[45] S. Höger, *Pure Appl. Chem.* **2010**, *82*, 821–830.

[46] The voids of the larger **MSW-1** and **MSW-2a/b** offered more room to accommodate larger parts of their alkyl chains. Furthermore, the peripheral alkyl chains adsorbed well on HOPG, thereby resulting in highly attractive alkyl–graphite interactions. Thus those com-

pounds could be visualized well by STM (ref. [10b]; K. Tahara, S. Lei, D. Mössinger, H. Kozuma, K. Inukai, M. Van der Auweraer, F. C. De Schryver, S. Höger, Y. Tobe, S. De Feyter, *Chem. Commun.* **2008**, 3897–3899; D. Mössinger, D. Chaudhuri, T. Kudernac, S. Lei, S. De Feyter, J. M. Lupton, S. Höger, *J. Am. Chem. Soc.* **2010**, *132*, 1410–1423). Such forces are missing in **MSW 3a/b**.

[47] W. Schärtl, *Light scattering from polymer solutions and nanoparticle dispersions*, Springer, Berlin/Heidelberg, **2007**.

[48] a) S. W. Provencher, *Comput. Phys. Commun.* **1982**, *27*, 213–227; b) S. W. Provencher, *Comput. Phys. Commun.* **1982**, *27*, 229–242.

[49] a) V. Privman, D. V. Goia, J. Park, E. Matijevic, *J. Colloid Interface Sci.* **1999**, *213*, 36–45; b) M. Y. Lin, H. M. Lindsay, D. A. Weitz, R. Klein, R. C. Ball, P. Meakin, *J. Phys. Condens. Matter* **1990**, *2*, 3093–3113; c) M. Y. Lin, H. M. Lindsay, D. A. Weitz, R. C. Ball, R. Klein, P. Meakin, *Phys. Rev. A* **1990**, *41*, 2005–2020; d) M. Y. Lin, H. M. Lindsay, D. A. Weitz, R. C. Ball, R. Klein, P. Meakin, *Nature* **1989**, *339*, 360–362.

[50] M. M. J. Smulders, M. M. L. Nieuwenhuizen, T. F. A. de Greef, P. van der Schoot, A. P. H. J. Schenning, E. W. Meijer, *Chem. Eur. J.* **2010**, *16*, 362–367.

[51] If desired, the corresponding phenol can be obtained by acid-promoted cleavage of the oxygen–carbon bond.

[52] S. Förster, L. Apostol, W. Bras, *J. Appl. Crystallogr.* **2010**, *43*, 639–646.

[53] S. Förster, S. Fischer, K. Zielske, C. Schellbach, M. Sztucki, P. Lindner, J. Perlich, *Adv. Colloid Interface Sci.* **2011**, *163*, 53–83.

Received: September 26, 2012
Published online: February 18, 2013

